Effects of Thymol Individually or Encapsulated in Chitosan Phosphate on the Properties of Poly(lactic acid) and Poly(butylene succinate) Matrix Reinforced with Nanofibrillated Cellulose

Nurul 'Afifah Zabidi,[a] Mohd Nazli Naim,[a] Siti Hajar Ariffin,[a] Hairul Abral,[b,c] Thinesh Sharma Balakrishnan,[d] and Intan Syafinaz Mohamed Amin Tawakkal [a,*]

* *Corresponding author: intanamin@upm.edu.my*

DOI: 10.15376/biores.21.3.8118-8156

GRAPHICAL ABSTRACT

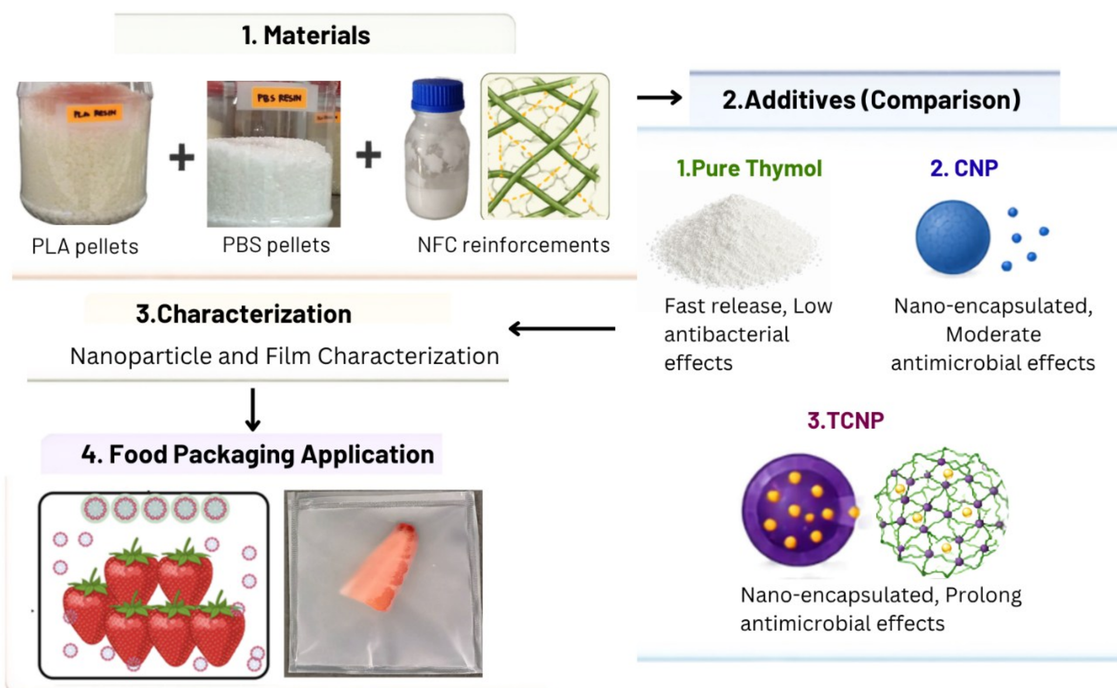

Effects of Thymol Individually or Encapsulated in Chitosan Phosphate on the Properties of Poly(lactic acid) and Poly(butylene succinate) Matrix Reinforced with Nanofibrillated Cellulose

Nurul 'Afifah Zabidi,[a] Mohd Nazli Naim,[a] Siti Hajar Ariffin,[a] Hairul Abral,[b,c] Thinesh Sharma Balakrishnan,[d] and Intan Syafinaz Mohamed Amin Tawakkal [a,*]

Thymol, a natural active compound, is recognized for its remarkable antimicrobial properties, making it a suitable choice for active agents in food packaging applications. This study focuses on the encapsulation of thymol in chitosan phosphate nanoparticles (CNP) to overcome its limitations, particularly volatility, and incorporates it into bio-nanocomposite films *via* solvent casting. Moreover, comparison of the effects of pure thymol, CNP, and encapsulated thymol-loaded chitosan phosphate nanoparticle (TCNP) on the film's properties were also assessed. The film's chemical interaction (Fourier transform infrared, FTIR), thermal, mechanical, light transmittance, water barrier, antibacterial, toxicity properties, and release test were evaluated. The results disclosed that the incorporation of 5 wt% of TCNP1.0 into the PLA/PBS/NFC films matrix improved thermal stability (0.76%), tensile strength (46.8%), and enhanced water barrier properties, as evidenced by a reduction in water vapor permeability (WVP) by 10.1%. The FTIR analysis demonstrated the presence of intermolecular hydrogen bonds, indicating the compatibility between TCNP and the PLA/PBS/NFC matrix. The bio-nanocomposite films also exhibited noteworthy antibacterial effects and had an inhibitory rate against *S. aureus*. In summary, bio-nanocomposite films have significant potential as an antibacterial agent in the advancement of innovative bio-based active packaging systems.

DOI: 10.15376/biores.21.3.8118-8156

Keywords: Bio-nanocomposites; Essential oil; Nanofibrillated cellulose; Poly (lactic acid); Poly (butylene succinate); Thymol

Contact information: a: Department of Process and Food Engineering, Faculty of Engineering, Universiti Putra Malaysia, 43400 Serdang, Selangor, Malaysia; b: Laboratory of Nanoscience and Technology, Department of Mechanical Engineering, Andalas University, Padang 25163, West Sumatera, Indonesia; c: Research Collaboration Center for Nanocellulose, BRIN-Andalas University, Padang 25163, West Sumatera, Indonesia; d: Laboratory of Biocomposites Technology, Institute of Tropical Forestry and Forest Products (INTROP), Universiti Putra Malaysia (UPM), 43400 Serdang, Selangor, Malaysia;
** Corresponding author: intanamin@upm.edu.my*

INTRODUCTION

Food safety and quality are the primary concerns of food producers and consumers. Food packaging is essential in this scenario to protect goods from physical damage, but it fails to suppress bacterial growth (Lu *et al.* 2021). Over the past few years, active packaging has garnered growing research interest in strengthening food cycle sustainability by preserving and extending food's shelf life (Basavegowda and Baek 2021). Commercial packaging currently employs non-degradable materials and synthetic additives, which may pose a safety risk and long-term environmental concerns (Jiang *et al.* 2025; Tan *et al.* 2025). Therefore, it is important to incorporate natural antimicrobial substances with renewable and biodegradable attributes (Shen *et al.* 2020) and demonstrate substantial potential in a wide range of applications.

Essential oils (EO) have garnered significant attention due to non-toxic, eco-friendly, and versatile properties (Assadpour and Mahdi Jafari 2019; Angane *et al.* 2022). Thymol emerges as a natural active compound, exhibiting characteristics of being colourless, crystalline, and monoterpenoid phenol abundant in plant *Thymus vulgaris* (Thyme), *Monarda* spp., and *Origanum* spp. (Sivaram *et al.* 2022). Research has shown that incorporating thymol in polymer matrices is particularly effective for antimicrobial effects, further extending their application in food preservation prospects (Chen *et al.* 2025; de Dicastillo *et al.* 2025). However, although thymol is endowed with effective antimicrobial properties, it is also prone to losing its antimicrobial effects when exposed to high temperatures or long-term storage, as it is challenging to incorporate it in packaging films. Thymol may undergo physical instability and lose its biological activity when exposed to harsh conditions (Alizadeh-Sani *et al.* 2021).

To address this issue, nanoencapsulation, particularly ionic gelation (IG), provides new routes to maintain stability and provide sustained release of EO under specific conditions (Almasi *et al.* 2021; Ferreira *et al.* 2021). Chitosan, a natural biopolymer consisting of N-acetyl D-glucosamine linked by β-1,4 linkage (Hasheminejad *et al.* 2019), is the most applied biopolymer and serves as an encapsulating agent in food preservation applications. Chitosan phosphate nanoparticles (CNP) are chitosan-based nanoparticles that are formed through the interactions of cationic chitosan with multivalent phosphate ions from sodium tripolyphosphate (STPP). Chitosan is widely utilized for ionic interactions due to its cationic nature ($pK_a = 6.5$) and the presence of free hydroxyl and amine groups, resulting in adequate interactions with the negative charge of STPP (Alehosseini *et al.* 2022). In fact, CNP has been widely researched and developed as a carrier for drugs and genes (Karam *et al.* 2020; Safer and Leporatti 2021; Mahmoud *et al.* 2024). The presence of a free amine group in CNP offers further cross-linking reaction and electro-potential to harness the stability of the developed nano-encapsulated thymol.

For practical application of active packaging technology, industrially compostable polymers, namely polylactic acid (PLA) and polybutylene succinate (PBS), are employed in this study as polymer matrices, given their degradability, renewability, and favourable functional properties (Bumbudsanpharoke *et al.* 2022; Wongphan *et al.* 2023). Nanofibrillated cellulose (NFC), resulting from the mechanical disintegration process of nanocellulose, was incorporated as a reinforcing material to PLA/PBS blends. On a positive note, the high aspect ratio and high density of covalent bonds per unit area of NFC contribute to enhanced crystallinity and high tensile strength (Abudula *et al.* 2019; Wu *et al.* 2019). In this study, PLA/PBS blends were reinforced with NFC to develop green packaging films with enhanced mechanical and ductility with sustainable biodegradation.

Although most of the previous studies had evaluated the efficacy of nano-encapsulated EO (Ferreira *et al.* 2021; Wang, X. *et al.* 2024) or provided comparisons with pure EO (dos Santos Paglione *et al.* 2019), or the interaction of the addition of CNP and pure EO (Vahedikia *et al.* 2019) in a polymer matrix. However, limited attention has been given to distinguishing the individual contribution of pure EO (thymol), nanoparticle carrier wall (CNP), and encapsulated EO (TCNP) toward the overall performance of films.

To date, Ferreira *et al.* (2023) have investigated the synergistic effect of nanocellulose and nano-encapsulated EO in poly (butylene adipate) (PBAT) films, demonstrating improvements in barrier properties, thermal stability, and antimicrobial activity. However, PBAT is a single-polymer matrix with physicochemical characteristics that differ from the PLA/PBS blend matrix. Furthermore, a limited study had systematically investigated the influence of NFC on the functional performance of polymer blend films containing thymol, CNP, and TCNP, focusing on active packaging applications. Therefore, understanding the interaction of NFC with these different active agents is important since NFC may alter the dispersion of active agents and consequently affect the properties of the resulting films.

PLA/PBS blends at 80/20 ratios, and 2 wt% NFC were selected because of demonstrated improvements in flexibility and thermal properties (Zabidi *et al.* 2023). Su, S. *et al.* (2019) stated that at a threshold of 20 wt% PBS, the blends exhibit partial miscibility, but with the ratios of 80/20, can improve the inherent brittleness by enhancing elongation at break (EaB). Furthermore, maintaining a high fraction of PLA (80 wt%) can ensure the structural integrity and dense polymer network (Garofalo *et al.* 2025). Moreover, Kargarzadeh *et al.* (2018) highlighted that the optimal loadings of nanocellulose (NC) were mainly in the range of 0.5 to 2 wt% for the compatible bonding between hydrophobic PLA and hydrophilic NC. Hanipa *et al.* (2026) reported that the addition of 1 wt% CNF *via* melt-blending, and Abdullah *et al.* (2019) observed that the incorporation of (1 to 5)wt% NFC by electrospinning enhanced the performance of PLA/PBS blends, which mainly were mechanical properties.

In the present study, IG techniques were proposed to encapsulate thymol in CNP, known as TCNP. Firstly, three CS: EO ratios were optimized to obtain small-sized and stable nanoparticles. Stable developed TCNP is important for the desired antimicrobial effects when incorporated in packaging materials. Subsequently, the optimized ratio of TCNP was incorporated into PLA/PBS reinforced NFC films, and their structural properties, thermal stability, and antimicrobial performance were investigated. Finally, highly perishable fruits were subjected to preservation analysis to assess the film's shelf-life extension capabilities. This study aims to provide not only biodegradable active packaging materials but also to ascertain the potential enhancements in the film's functionality resulting from the encapsulation process.

EXPERIMENTAL

The present study aimed to encapsulate thymol on the nanoscale to enhance the film-forming properties together with antibacterial effectiveness. Chitosan was chosen as a wall material for encapsulating thymol due to its compostability and biocompatibility. That was followed by the fabrication of nanoparticles by the ionic gelation method. There were three different mass ratios of chitosan: thymol, namely as 1:0.4 (TCNP0.4), 1:0.8 (TCNP0.8), and 1:1 (TCNP1.0). Both CNP and TCNP were characterized for their particle size and polydispersity index (dynamic light scattering, DLS), encapsulation efficiency (ultraviolet-visible, UV-vis spectrometry), and morphological (transmission electron microscopy, TEM). Then, the chemical interactions of pure thymol, CNP, and three mass ratios of TCNP were assessed by FTIR analysis. Subsequently, three different concentrations (3, 5, and 7 wt%) of pure thymol, CNP, and three mass ratios of TCNP were incorporated into PLA/PBS and PLA/PBS/NFC films and were further characterized by mechanical and quantification analysis.

Materials

Polylactic acid (PLA) pellets (type 7001D, MFR = 6 g/10 min, specific gravity = 1.24 g/cm^3) were obtained from Nature Works (USA). Biobased polybutylene succinate (PBS) (type FD92PM/PB, MFR = 4 g/10 min, specific gravity = 1.24 g/cm^{3}) was procured from PTT MCC Biochem CO. (Bangkok, Thailand). Chitosan (≥ 75% deacylated) was purchased from Sigma Aldrich. Nanofibrillated cellulose (NFC) derived from palm oil Empty Fruit Bunch (EFB) was obtained from Zeopnano Sdn. Bhd., Malaysia with a size of < 80 nm. Anhydrous calcium chloride, chloroform, glacial acetic acid, thymol, Tween 80, sodium tripolyphosphate (STPP), and magnesium nitrate were obtained from R&M Chemicals, Malaysia.

Synthesis of TCNP

Thymol encapsulated in CNP, which were prepared by IG techniques. Wang X. *et al.* (2022), and Oluoch *et al.* (2021) have reported this approach to provide a sustained release effect. Encapsulated thymol-loaded chitosan phosphate nanoparticle (TCNP) was prepared through the process of ionic gelation (IG), with a modification based on previous research conducted by Zhang *et al.* (2019), who previously reported successful encapsulation of *Paulownia Tomentosa* EO in CNP with a mean diameter of 180 nm. A solution of chitosan (3.2 mg/mL) was prepared at 65 °C for 30 min. Subsequently, any undissolved chitosan particles were filtered through a 1 µm pore size. The pH of the chitosan solution was calibrated to a range of 4.7 to 4.8. Following this, 100 mg of Tween-80 was mixed with the above solution while being continuously agitated for 30 min at 60 °C to form a uniform emulsion. Thymol was incorporated dropwise into the solution by varying three chitosan to thymol weight ratios: TCNP0.4, TCNP0.8, and TCNP1.0 while stirring continuously at 1300 rpm for 30 min. Subsequently, 1.88 mg/mL of STPP was gradually incorporated into chitosan/EO emulsion with mild agitation for 1 h. The wet pellets of TCNP were acquired *via* centrifugation for 30 min at 9,000 rpm and rinsed three times with distilled water. These suspensions were immediately dried at −65 °C for 72 h by a freeze dryer for the thermal stability analysis. Silva *et al.* (2025) stated that the first indication of successful encapsulation of active compounds in CNP was by physicochemical changes, which mainly include size and zeta potential changes. Therefore, the obtained TCNPs were characterized based on the mean particle size, polydispersity index, zeta potential (ZP), encapsulation efficiency, morphology, FTIR, and thermal stability analysis.

Preparation of Active Bio-nanocomposite Films

Active bio-nanocomposite films were prepared using the solvent casting method. PLA and PBS were dissolved separately in chloroform with a ratio of 80/20 and stirred for 2 h. Subsequently, both solutions were mixed, and a fixed loading of NFC (2% wt%) was added and stirred for another 4 h. Different concentrations (3, 5, and 7% wt%) were dissolved for the formulations with pure thymol, wet pellets of CNP, and TCNP. The film's forming solution was cast on a glass petri dish and dried for 48 h in fume hoods, and the films were peeled after the solvent had volatilized. The prepared films were stored at 25 °C and 50% relative humidity (RH) for further use.

Particle Size and Physical Characterization of TCNP

The mean particle size, polydispersity index, and zeta potential (ZP) of CNP and TCNP were determined by the dynamic light scattering (DLS) technique using a Zetasizer Particle Analyzer (NanoPlus, Japan). The encapsulation efficiency (EE) of TCNP was determined using the UV-Vis spectrophotometer (Thermo Scientific Biomate 160, USA). Freshly prepared TCNP wet pellets (200 µL) were mixed with 2 mol/L of 5 mL of HCL solution and refluxed for 30 min. It was then cooled down, and 2 mL of absolute ethanol was added, followed by centrifugation (9000 rpm for 5 min) (Zhang *et al.* 2019). The obtained supernatant was then transferred for spectrometer analysis, and the absorbance was measured at wavelengths ranging from 250 to 350 nm. A maximum UV-Vis absorption wavelength for pure thymol was obtained at 274 nm. The supernatant was diluted in pure ethanol, and the amount of loaded thymol in CNP was quantified using a calibration curve of pure thymol in ethanol (R^2=0.996) (Garcia-Salazar, G. *et al.* 2026). Control CNP suspension was used as a blank. The EE was calculated using Eq. 1 (Kaboudi *et al.* 2023).

$$\text{EE (\%)} = \frac{amount\ of\ loaded\ Thymol\ in\ CNP}{initial\ amount\ of\ Thymol}\ x100 \quad (1)$$

TEM Observation

The morphology of both CNP and TCNP was examined using a Transmission Electron Microscope (TEM-JEOL 2100, Japan). For this purpose, a drop of suspension was deposited on a copper grid. The observation was performed at an accelerating voltage operating at 200 kV. The determination of average particle size was accomplished by employing the ImageJ software (Sotelo-Boyás *et al.* 2017).

Fourier Transform Infrared (FTIR) Spectroscopy

The FTIR analysis was used to study the chemical structure elements of the pure thymol, CNP, TCNP, and the prepared films. The FTIR spectra were studied in a range of 4000 to 400 cm^{-1}, featuring a resolution of 4 cm^{-1}, while the scanning frequency operated at 32 times per minute.

Thermal Stability

Thermal properties of TCNP and active films were characterized using a TA analyser (TGA 4000, Perkin Elmer, USA). For this analysis, freeze-dried TCNP (5 to 8 mg) and active films (8 to 12 mg) were analysed at heating temperatures in the range of 25 to 500 °C, at a rate of 10 °C/ min. All film samples were subjected to three parallel runs.

Film Characterization

The mechanical properties were assessed utilizing an Instron Universal Testing Machine in accordance with the testing protocol outlined in ASTM D882-10 (2010). The film's specimens were conditioned under 51% RH at 25°C for 24 h before testing. Then, the film's samples were cut into a rectangular shape with dimensions of 100 x 15 mm by using a Cutter Press. Five replications of the film sample were tested at a crosshead speed of 5 mm/min and a grip distance of 50 mm (Laorenza *et al.* 2026). The average value was calculated using the equation described by Wang, Y. *et al.* 2025.

$$\text{Tensile strength (MPa)} = \frac{F}{W \times d} \quad (2)$$

$$\text{Elongation at Break (\%)} = \frac{\Delta L}{L} \times 100\% \quad (3)$$

where F is the fracture strength (N); w is the sample width (mm); d is the film thickness (mm), ΔL is the total deformation (mm) and L is the original scale length (mm).

To check the amount of thymol content remaining in films, a preliminary release assay was conducted to analyse the required time for thymol to be fully released from the films, as referred to in Sáez-Orviz *et al*. (2020). A 12 cm² of film was placed in 20 mL of 95% ethanol at 45 ºC for 48 h. A total of 3 mL of an aliquot was taken several times and measured at the UV-vis absorption wavelength of 274 nm. Thymol concentration was analysed in comparison to a standard curve (R^2 = 0.9908) with films without thymol as a blank. The amount of thymol released into the ethanol was compared with the amount of thymol incorporated into the film-forming solution to calculate the thymol loss during the drying step. The FTIR analysis and thermal stability of selected films were evaluated using the same equipment and procedure described earlier.

Properties for Food Packaging Applications

This section focuses on assessing the functional properties that are relevant to food packaging applications. The analysis includes the water barrier (WVP), which determines the film's barrier effectiveness against moisture, and light transmission to assess the film's ability to protect food from UV and visible light exposure. Moreover, it includes a liquid culture assay to examine the potential of films to inhibit microbial growth and a toxicity assay to assess the safety and effectiveness in extending food's shelf-life.

Water vapor permeability and light transmittance

The water vapor permeability (WVP) was measured following the gravimetric method ASTM E96-95 (1995) by using a water vapor permeability cup (Yasuda, No. 318 Japan) according to the JIS Z 0208 (1976) method. The cup was filled with 10 g of anhydrous calcium chloride, then covered with films and placed in a desiccator containing saturated magnesium nitrate solutions, ensuring a stable RH of 51% at a temperature of 25 °C. The cup's weight was recorded at 24-h intervals. The water vapor transmission (WVTR) was assessed through the gradient of weight variations over time, divided by the surface area of the cup mouth (m^2). Afterward, the WVP was computed following Eq. 4. The light transmission properties of the films were measured using the Hunter LAB Ultra Scan VIS 8 Spectrophotometer (Ultra Scan Pro USP 1431, USA). in the visible region (360 to 780 nm), following the guideline set forth in Othman *et al.* (2019),

$$\text{WVP} = (\text{WVTR} \times \text{L}) / (P_1 - P_2) \quad (4)$$

where L is the average thickness of the film (mm), P_1 is the water vapor partial pressure in the desiccator at RH of 51%, 21.64 × 10^5 Pa, and P_2 is the water vapor partial pressure in the cup at RH of 0 Pa.

Antibacterial properties

The antibacterial properties of films were evaluated using a method adapted from Sun *et al.* (2024) with some modifications. The antibacterial agents were tested against two strains of Gram-positive (*S. aureus*) and Gram-negative (*E.coli*) bacteria acquired from the Microbiology Laboratory, Department of Food Science and Technology, UPM, Malaysia.

A total of 0.1 mL of bacterial suspension was inoculated into nutrient broth containing pure thymol, CNP, TCNP1.0, and film samples (cut into pieces), followed by incubation at 37 °C for 24 h. The cultivated bacteria were then subjected to sequential dilution in 9 mL of 0.1% sterile peptone water. Following this, 0.1 mL of diluted series (approximately 10^5) was spread on PCA agar and then incubated at 37 °C for 24 h.

Toxicity assay

To assess the safety of applying active bio-nanocomposite films, the assessment of cytotoxicity was completed utilizing the MTT (2,5-diphenyl-3, -(4,5-dimethyl-2-thiazolyl) tetrazolium bromide) on 3T3 fibroblast cell lines (Boeira *et al.* 2022; Cheng *et al.* 2022). The cells were seeded at a density of 3000 cells/well and then incubated in 96-well plates containing DMEM for 24 h. Subsequently, film samples with an 8 mm diameter were positioned at the hole's base to interact with the 3T3 fibroblast cell lines directly. After 48 h of treatment, the film samples were removed and washed with phosphate buffer saline three times. Post rinsing, 100 µL of MTT (at a final concentration of 0.5 mg/mL) was added to each well, and the plates were left to incubate for 4 h. The absorbance readings at 570 nm were recorded using a microplate reader, with a 100% cell viability group serving as the reference point, denoted by the blank control group.

Thymol release test in food simulants

The release of thymol from PLA/PBS and PLA/PBS/NFC films was evaluated by using 95% v/v ethanol (Simulant D2- fatty foods), in agreement with EU regulations, which state that the migration behavior of additives can be investigated by replacing real foods with food simulants (Li, B. *et al.* 2025; European Commission, 2011). The films (12 cm^2) were placed in amber vials filled with 20 mL of food simulants. The area-to-volume ratio was 6 dm^2/L at 45°C in an oven (Ramos *et al.* 2025). The samples were then evaluated by using the UV-Vis spectrophotometer (Thermo Scientific Biomate 160, USA) (Ferreira *et al.* 2023), using a wavelength of 274 nm, and were performed for 96 h. After measurement, the ethanol sample was returned to the vials (Sáez-Orviz *et al.* 2020). The measurement was conducted in duplicate.

Packaging films with strawberry

Fresh strawberries were packaged with active films PLA/PBS, and PLA/PBS/NFC incorporated with CNP, pure thymol, and TCNP. They were stored and maintained at 4 ºC for 5 days to mimic the local storage conditions. The appearance and daily change in sample weight were recorded and photographed, and the weight loss was calculated using Eq. 5 (Huang *et al.* 2023). W_1 and W_2 are the weights of the samples before and after the different storage stages, respectively:

$$\text{Weight loss (\%)} = \frac{W1-W2}{W1}\ x\ 100 \tag{5}$$

Statistical Study

The experimental data presented were analysed using analysis of variance (ANOVA) to evaluate the significant difference between means. Tukey's test was subsequently applied to compare the means, with statistical significance determined at a threshold of $p < 0.05$. The statistical analysis was conducted utilizing Minitab Software (Minitab Inc., version 16, State College, PA, USA).

RESULTS AND DISCUSSION

DLS Measurements

Table 1 displays the average particle size of TCNP loaded at various CS: EO ratios. According to literature, DLS techniques measure the fluctuations in scattered light intensity to determine particle sizes and are widely used in fields such as food science and pharmaceuticals (Tosi *et al.* 2020; Kirichenko *et al.* 2021). The polydispersity index (PDI) is a key measure of particle distribution in suspension (Hasani *et al.* 2018). An unloaded CNP showed a slightly smaller size (158 nm) and a lower PDI than the loaded CNP. Specifically, after incorporating thymol, the diameter of TCNP at mass ratios of TCNP0.4 and TCNP0.8 was slightly larger, measuring 317 and 246 nm, respectively. Results indicate that at higher thymol loading (TCNP1.0), the size was smaller compared to other formulations. Russo *et al.* (2014) demonstrated that smaller particle sizes indicate denser packing of polymer chains, which facilitates the interaction of active compounds and influences TCNP size. Furthermore, smaller sizes have been linked to ratios of entrapment compounds (Hasani *et al.* 2018). Conversely, for TCNP0.4 and TCNP0.8, which contain higher chitosan content, the presence of more amino groups in chitosan results in a larger diameter. Abushal *et al.* (2025) reported that the increase in nano-capsule size after encapsulation primarily occurs because bioactive thymol adsorbs onto the surface and is contained within the nano-capsule, leading to enhanced ionic cross-linking and increased protonation of amino groups (Hasheminejad *et al.* 2019; Zhang *et al.* 2019).

A similar observation was noted upon the encapsulation of EO. Zhang *et al.* (2020) obtained the average diameter of tarragon EO-NPs ranging from 333 to 505 nm. Hadidi *et al.* (2020) observed the enlargement of clove EO-loaded chitosan NPs with the increasing chitosan/CEO ratio, with an average mean diameter in the range of 223 to 444 nm. Results showed that the PDI falls within the range of 0.174 to 0.275, indicating the monodisperse populations with homogeneous distribution (Barrera-Ruiz *et al.* 2020). Moreover, Table 1 shows that higher thymol loading (TCNP1.0) corresponded to the highest zeta potential (ZP) (17.4 mV), whereas lower thymol loading (TCNP0.4) exhibited the lowest ZP value (10.6 mV). Generally, ZP values higher than 30 mV indicate high physical stability, values around 20 mV correspond to short-term stability, and values lower than 5 mV have low stability and fast aggregation (Soltanzadeh *et al.* 2021; Kaboudi *et al.* 2023). In another study, chitosan NPs and cinnamon EO-loaded chitosan NPs were reported to have positively charged surfaces due to the presence of amine groups; zeta potential values were +24.0 mV and +26 to +30.5 mV, respectively (Matshetshe *et al.* 2018). In a study by Hasani *et al.* (2018), the values of zeta potential for chitosan-Hicap nano-capsule containing lemon EO ranged from +10.6 to +44.2 mV. However, it can be observed that the ZP of non-loaded CNP was higher (18.0 mV) than that of loaded CNP. The decrease in zeta potential value resulted from less availability of free amine groups on the surface of NPs due to the possible interaction between them and EO (Sotelo-Boyás *et al.* 2017).

Zeta potential (ZP) reflects the net electrical charge of particles. As shown in Table 1, TCNP exhibited positive values of ZP. STPP carries on multivalent phosphate ions (PO_4^{3-}), which mainly act as an internal crosslinker with the protonated amine group of chitosan within the nanoparticle core. Therefore, the outer surface remains enriched with the residual protonated amine group of chitosan and forms a shell-like structure, as shown in Fig. 1. This explanation can be supported by Silva *et al.* (2025), who stated that encapsulation of active compounds in CNP *via* IG typically exhibits positive values for ZP due to protonation of $–NH_3^+$ groups.

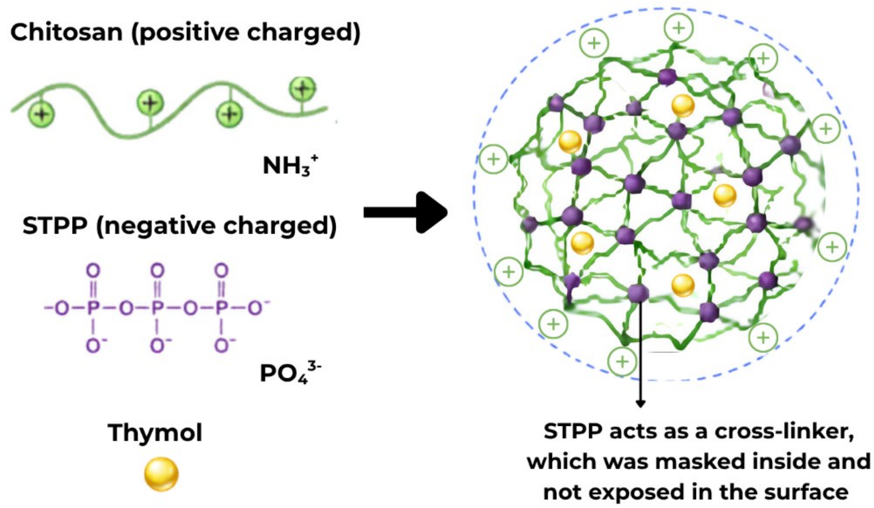

Fig. 1. Schematic illustration of the positive charges of the zeta potential of TCNP

Table 1. Mean Particle Size, PDI, Zeta Potential, and Encapsulation Efficiency of CNP and TCNP

Nanoparticle	Particle Size (nm)	PDI	Zeta Potential (mV)	EE (%)
CNP	158.1 ± 8.68^{a}	0.174 ± 0.033^{a}	18.01 ± 0.75^{c}	-
TCNP0.4	316.9 ± 4.74^{c}	0.275 ± 0.013^{b}	10.64 ± 1.51^{a}	38.5 ± 0.77^{a}
TCNP0.8	245.9 ± 4.49^{b}	0.184 ± 0.025^{ab}	$12.61 \pm 0.^{19ab}$	42.2 ± 1.62^{b}
TCNP1.0	187.8 ± 5.41^{ab}	0.217 ± 0.006^{b}	17.39 ± 0.2^{b}	53.5 ± 2.39^{c}

Means with the column followed by different superscripts are significantly different at $p \leq 0.05$

Encapsulation Efficiency

The encapsulation efficiency (EE) is shown in Table 1. The values for EE ranged from 38.5 ± 0.77 to 53.5 ± 2.39 and increased significantly ($p < 0.05$) with the increase in thymol content. The lowest EE was obtained in CS: EO ratios (TCNP0.4). This could be explained by the lower thymol concentrations that may have formed larger particle sizes, negatively impacting EE. Kazeminia *et al.* (2024) stated that larger-sized nanoparticles were located externally, which caused the loosened attachment of EO on the surface of larger nanoparticles. This phenomenon may lead to the detachment of EO during processing, which significantly reduces encapsulation efficiency (Corrado *et al.* 2022). Moreover, lower loading thymol was observed to have lower ZP values, which may have caused an aggregation and consequently reduced the EE (Kazeminia *et al.* 2024). In the present study, the higher CS: thymol ratio (TCNP1.0) was shown to have higher EE (53.5%) compared with other formulations (1:0.4 and 1:0.8). A recent study by Wang, X. *et al.* (2022) stated that encapsulation of thymol in chitosan phosphate nanoparticles at a 1:1 ratio facilitates the maximum EE. Moreover, similar observations have been reported by Esmaeili and Asgari (2015), who also strongly support this finding, demonstrating that a 1:1 chitosan to *Carum copticum* essential oil (CEO) ratio possessed the maximum EE, but decreased at a ratio of 1:1.25 weight ratio of chitosan to CEO. These findings suggested that excessive loadings of EO may exceed the capacity of encapsulations and reduce the entrapment efficiency.

TEM Observations

Figure 1 shows transmission electron microscopy (TEM) images of non-loaded CNP and thymol-loaded chitosan nanoparticles (TCNP0.4, TCNP0.8, and TCNP1.0) at different CS: EO ratios. The micrographs displayed with scale bars of 200 and 100 nm clearly illustrate the influence of loading thymol into CNP on the morphological and size distribution of the nanoparticles. Higher magnification yields more microstructural details compared with images captured at lower magnification. At a 100 nm scale bar (Fig. 2B), CNP showed spherical particles with some degree of aggregation, but in 200 nm scale bars (Fig. 2A), more CNP nanoparticles appeared to be clustered together. The CNP often has a pronounced tendency to aggregate and cluster, potentially indicating the absence of thymol, which impacts the stability of CNP, as observed by Velderrain *et al.* (2019). Moreover, Pant and Negi (2018) suggested that inter and intra-crosslinking between TPP molecules with the amino groups of chitosan resulted in the irregular shape of CNP.

Upon incorporation of thymol, notable morphological changes for TCNP0.4, TCNP0.8, and TCNP1.0 were observed. The nanoparticles (Figs. 2E and 2G) show a denser and darker morphology in the image taken at 200 nm magnification, reflecting the successful encapsulation of thymol. These findings were supported by Russo *et al.* (2014) and Ziaee *et al.* (2023). It can also be seen that TCNP0.4 (Fig. 2C and 2D) tended to form aggregated particles. Herdiana *et al.* (2024) stated that low content of EO with high polymer concentration may cause the alteration of surface charge or electrostatic stabilization, which possibly reduces repulsion between particles and increases chances of aggregation. Moreover, it can be observed that TCNP0.8 (Fig. 2F) tends to form a slightly irregular outline and large particles, which may correspond to chitosan surrounding the encapsulated thymol. Rajivgandhi *et al.* (2023) suggested that TEM images of encapsulated EO showed a ball-like structure when it was clearly covered by a chitosan layer. Furthermore, it was previously stated that the formation of large aggregate particles as a result of lower loading of thymol caused the free oil molecules to adhere to the surfaces of NPs, which led to the instability of NP (Yang *et al.* 2021; Kaboudi *et al.* 2023).

Meanwhile, higher amounts of thymol (TCNP1.0) (Fig. 2H) showed stable and spherical individual particles, indicating successful synthesis at the nano scale with an average diameter of 33 to 64 nm. Most studies report that increasing EO content, such as clove EO (Hadidi *et al.* 2020), lemongrass EO (Soltanzadeh *et al.* 2021), *Carum copticum* EO (Ziaee *et al.* 2023), and *Piper nigrum* EO (Rajkumar *et al.* 2020), generally leads to larger and more aggregated particles. However, Kazeminia *et al.* (2024) observed that *Ziziphora clinopodioides* L. EO exhibited a decrease in particle size with increasing EO content, which was likely due to the optimized nucleation, interfacial stabilization, and specific polymer oil interactions. The TEM results are in line with the dynamic size distribution obtained from DLS measurements, which show that increasing the thymol loading significantly reduced the particle size. Similarly, in the current study, TCNP1.0 had smaller, spherical, and less aggregated particles, suggesting that higher thymol loadings enhanced interfacial stabilization and strong electrostatic forces between thymol and chitosan matrix. These forces may prevent volatile thymol molecules from evaporating from the chitosan matrix.

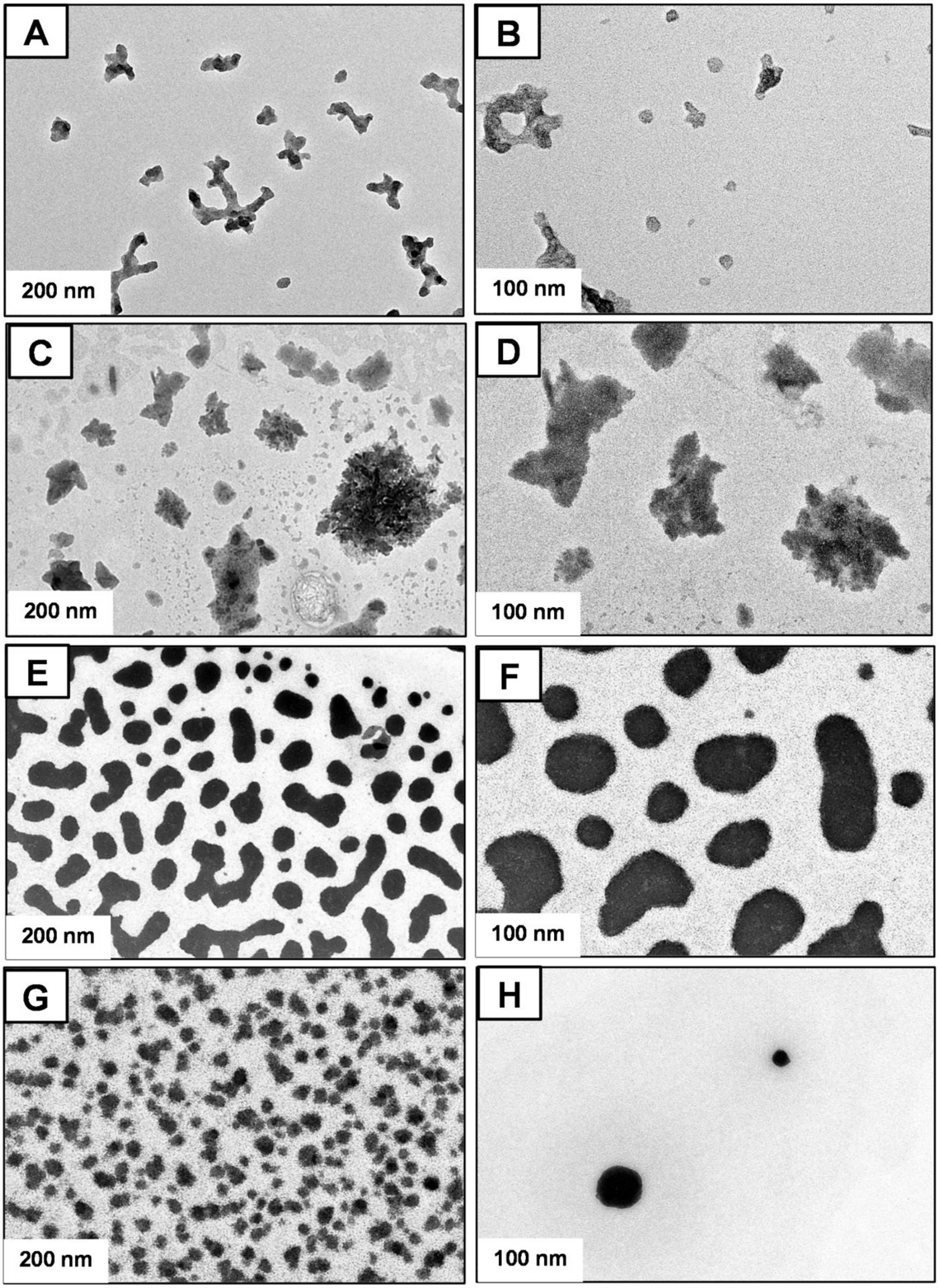

Fig. 2. TEM observations of (A, B) non-loaded (CNP), (C, D) TCNP0.4, (E, F) TCNP0.8, and (G, H) TCNP1.0

Hajibonabi *et al.* (2023) stated that nanosized droplets of bioactive compounds can significantly enhance their solubility and bioavailability. Additionally, the reduction in droplet sizes can improve the interfacial stabilization, which helps to mask the strong odors and reduce the volatility (Ozogul *et al.* 2022), causing less effect on the food's sensory qualities (de Oliveira Filho *et al.* 2021). Besides, Saifullah *et al.* (2016) stated that tiny droplets of nano-emulsions may also affect the mouthfeel and texture of products.

Thymol is known for its characteristics to have a strong odor and a pungent taste. While encapsulation may mask the odor, optimization of formulation is essential to minimize the adverse sensory effects and guarantee customer approval (Ozogul *et al.* 2025). A previous study reported that thymol nano-emulsion coatings, in an oil phase composition, had 45% of thymol and 55% a medium-chain triglyceride (MCT) oil. These results indicate a slow release of aroma and improve sensory acceptance of strawberry by day 12 compared with unencapsulated thymol (Robledo *et al.* 2018).

FTIR of TCNP

Further studies were conducted by FTIR analysis to explore the chemical interactions of primary functional groups implicated in the CNP, pure thymol, and TCNP1.0, as shown in Fig. 3. Pure thymol exhibited a characteristic peak at 3501 cm^{-1} (OH stretching), characteristic peaks at 3003 cm^{-1} (CH stretching), 1755 cm^{-1} (C=O stretching), 1094 cm^{-1} (C-O-C stretching), and 866 cm^{-1} related to the stretching vibration and bending vibration absorption of the C-H bond in the benzene ring (Zhao *et al.* 2023; Zikeli *et al.* 2023). The CNP showed a characteristic broad peak absorption at 3361 cm^{-1}, indicating the hydrogen-bonded O-H stretch band in chitosan. This showed that lignin sterols, alkaloids, hydroxyl, amine, alcohol, phenol, and carboxylic acid functional groups are among the proteins and secondary metabolites that surround chitosan (Anand *et al.* 2018). Further, the bands at 1639 cm^{-1} correspond to the C=O stretching of the amide I, confirming the hydrostatic interaction involving the amine group of chitosan and the phosphoric groups in sodium tripolyphosphate (STPP). The other prominent bands appeared at 1371 cm^{-1}, assigned to CH_3 symmetrical deformation. These results were in agreement with a previous study (Shetta *et al.* 2019; Alehosseini *et al.* 2022).

The FTIR spectra of TCNP for all mass ratios exhibited the characteristic functional groups of CNP and pure thymol. The presence of this absorbance peak indicated the presence of thymol within the chitosan matrix. Therefore, FTIR results are consistent with the presence of thymol in TCNP formulations (El-Aziz *et al.* 2018; Shetta *et al.* 2019). It should be noted that a new peak appeared at 1550, 1542, and 1539 cm^{-1} in TCNP0.4, TCNP0.8, and TCNP1.0 for amide II respectively, which might be due to the interaction formed between CS and TPP by ionic bonds (Alehosseini *et al.* 2022). The increasing intensity of symmetrical deformation CH_3 at peak 1371 cm^{-1} was probably due to an increase in polarization of the carbonyl group upon interaction of thymol and CNP (De Carvalho *et al.* 2019). A noticeable enhancement in the intensity of the ether (C-O-C) bonds at 1755 and 1094 cm^{-1}, indicating a possible interaction or enhancement of hydrogen bonding (Alehosseini *et al.* 2022). Furthermore, after incorporation of thymol into CNP, the distinctive band at 1094 cm^{-1} became wider with a slight shift towards lower wavenumbers in comparison with the CNP with TCNP1.0, which exhibited the lowest wavenumber (1086 cm^{-1}), suggesting an intermolecular hydrogen interaction between the OH groups.

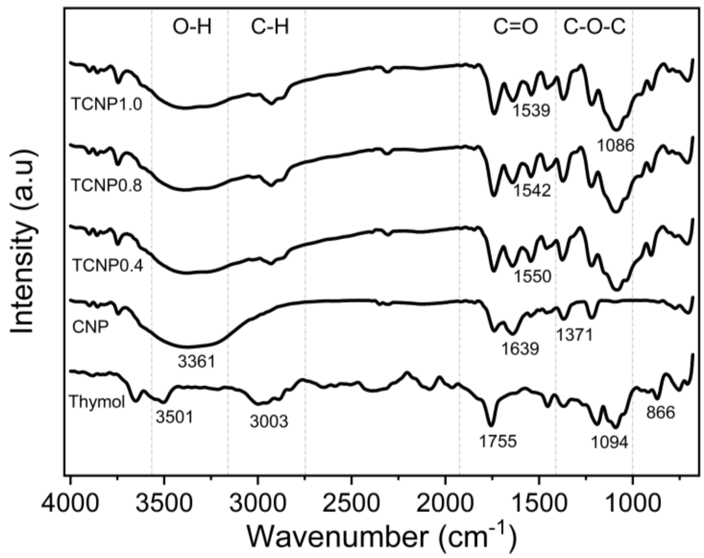

Fig. 3. The FTIR spectra of CNP, pure thymol, and TCNP

Thermal Stability of TCNP

To further characterize the optimal loading for TCNP, thermogravimetric analysis (TGA) was employed to examine the thermal properties of a freeze-dried sample, as depicted in Fig. 4. Thermogravimetric (TGA) analysis was performed to measure the change in TCNP mass as it is heated under controlled temperature from 25 to 500 °C. TGA analysis was primarily used to evaluate their resistance to decompose. TCNP0.8 and TCNP1.0 exhibited a three-step weight loss, whereas TCNP0.4 showed a four-step process. The first step, occurring from 40 to 80 °C, was attributed to the removal of water and moisture from the sample surfaces. Additionally, TCNP0.4 showed a new one-step mass loss starting at 162 °C, likely due to the decomposition of pure thymol adsorbed on the surface of CNP, consistent with Shetta *et al.* (2019), who found that decomposition of free green tea essential oil (GTO) adsorbed on the surface of CS/GTO NPs occurs at 130 to 140 °C. This event may also be related to the larger size of TCNP0.4 observed in TEM images, because larger particles tend to have lower stability and possibly more cracks and pores, which could allow pure thymol to escape more quickly at higher temperatures. Meanwhile, the other two mass ratios (TCNP0.8 and TCNP1.0) did not show any peaks in this temperature range.

The next step was attributed to the decomposition of sodium tripolyphosphate (STPP)-linked chitosan phosphate nanoparticles (CNP), corresponding to 250 to 300 °C (Hadidi *et al.* 2020; Soltanzadeh *et al.* 2021). The final thermal event was observed at range *T* = 300 to 400 ºC. This stage represents the interaction between thymol and CNP, which promotes the enhancement of thermal stability in TCNP. Similar findings have been reported for encapsulating EO in CNP (Shetta *et al.* 2019; Hadidi *et al.* 2020; Soltanzadeh *et al.* 2021). Comparing all three mass ratios, TCNP1.0 exhibited the highest degradation temperature at 367 ºC, indicating the encapsulation improves the thermal resistance of TCNP1.0 by delaying the degradation under high temperatures, reflect from the TGA analysis. Smaller particles generally have a more compact structure and less porosity, limiting their diffusion, which slows the release of thymol at high temperature. Thus, the nano-sized TCNP1.0 was selected for incorporation into PLA/PBS and PLA/PBS/NFC films.

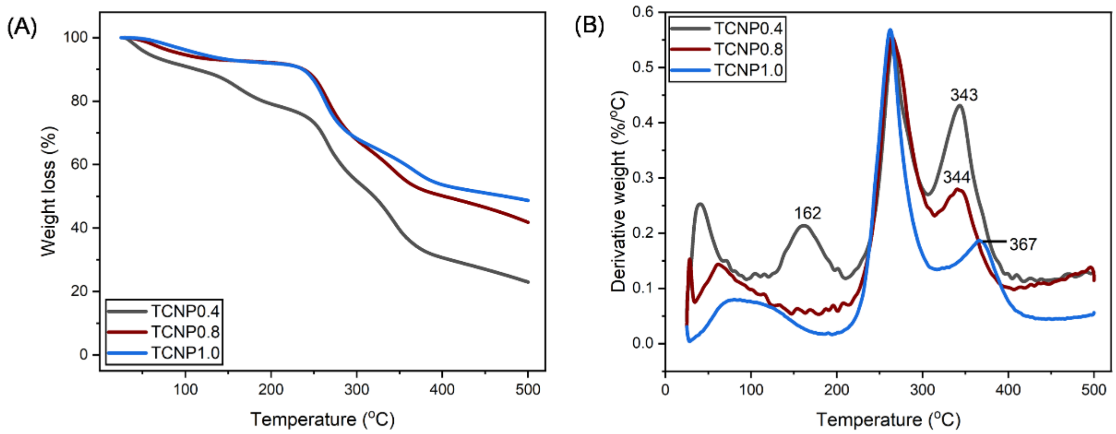

Fig. 4. Thermograms of TCNP at three mass ratios (A) TGA and (B) DTG

Active PLA/PBS and PLA/PBS/NFC Films' Properties

Mechanical properties

Mechanical properties, including tensile strength (TS) and elongation at break (EaB), are important parameters when evaluating biodegradable packaging materials for active packaging applications. Figure 5 shows the mechanical properties of films. The neat PLA/PBS film has TS, EaB, and tensile modulus (TM) of about 14.7 MPa, 9.24%, and 563 MPa, respectively. Meanwhile, PLA/PBS/NFC films exhibited 16.7 MPa, 8.5%, and 646 MPa. At 3 wt% of incorporation of CNP, pure thymol and TCNP, the TS and EaB values were reduced, possibly due to the low loading of the nanoparticle, and thymol may not yet be sufficient to interrupt polymer entanglement, which leads to lower intermolecular interaction that consequently reduces TS and EaB values. Additionally, lower loading of nanofillers can weaken interphase adhesion and reduce stress-transfer efficiency across blend phases, which reduces the mechanical properties of films (Dadashi *et al.* 2025). Wang, Y. *et al.* (2023) also observed that the addition of low polydopamine encapsulated EO nano-capsules significantly reduced the mechanical properties of soy protein isolate-carboxymethyl cellulose (SPI-CMC) films. However, Garavand *et al.* (2022) incorporated the CNP in whey-based poly (l-lactic acid) (PLLA) films and found that the addition of CNP up to 3 wt% increased TS and TM, but any further increase in the amounts resulted in low TS and TM.

At 5 wt% loading, the addition of CNP increased the TS and EaB value of PLA/PBS films but reduced the TS value of PLA/PBS/NFC films. The incorporation of CNP led to a pronounced TS value of PLA/PBS films, indicating enhanced stiffness and effective stress transfer through the hydrogen bond formed with the PLA/PBS matrix.

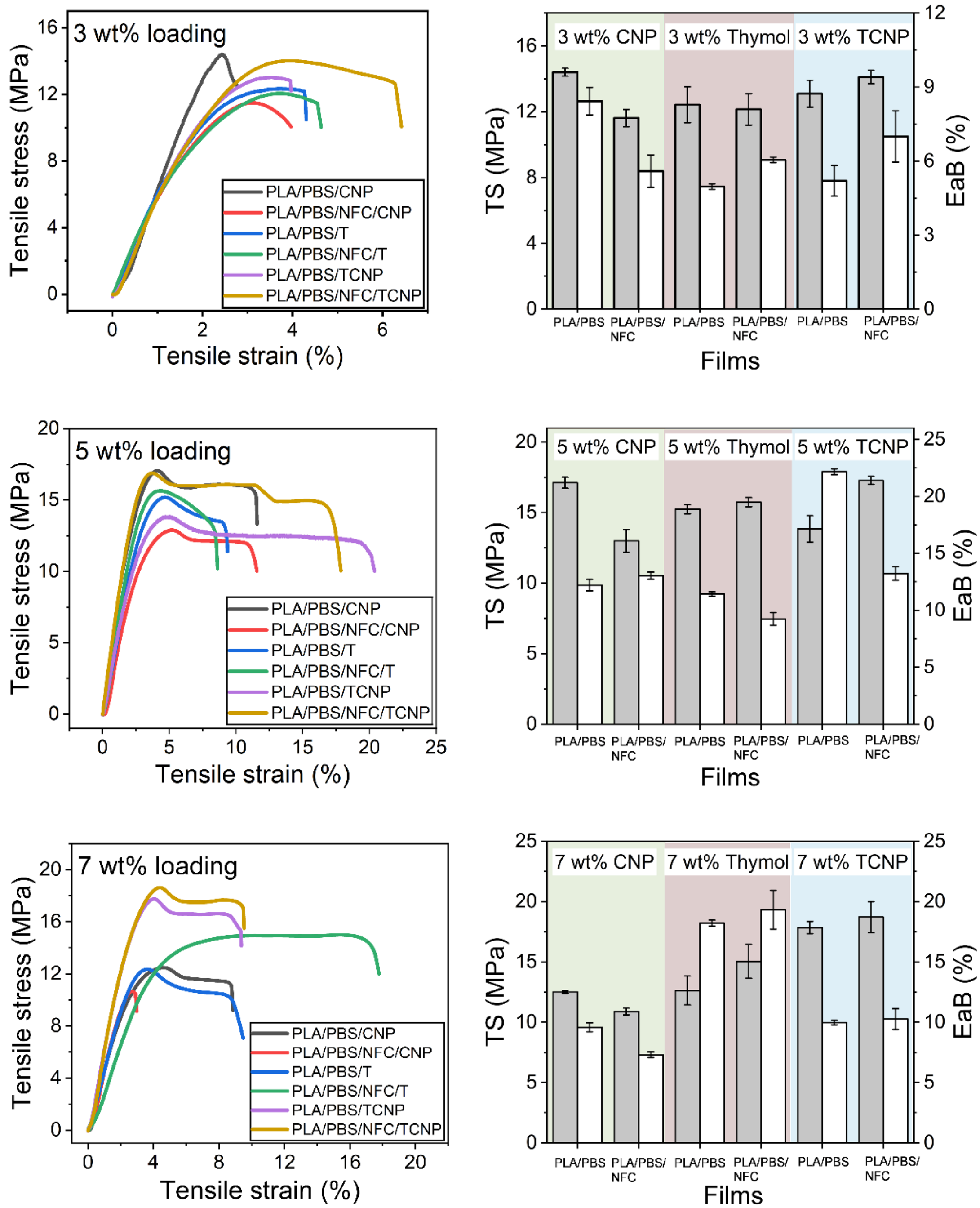

Fig. 5. Mechanical properties of PLA/PBS and PLA/PBS/NFC films incorporated with three concentrations (3, 5, and 7 wt%) of CNP, pure thymol, and TCNP

Moreover, Gomathi *et al.* (2017) noted through TGA analysis that CNP synthesized *via* ionotropic gelation exhibits a higher water weight loss percentage compared to chitosan. This is possibly due to the CNP's higher hydrophilicity, which in this case consequently reduced the mechanical properties of PLA/PBS/NFC films. However, the addition of pure thymol slightly reduced the TS value but increased EaB values of PLA/PBS and PLA/PBS/NFC films due to the plasticizing effects, which can be attributed to stronger molecular interactions. In contrast, addition of 5 wt% of TCNP1.0 led to an increase of TS and EaB values of PLA/PBS and PLA/PBS/NFC films. Regarding the TCNP1.0 nano-capsule, wherein both chitosan and thymol possess hydroxyl groups, there appeared to be a significant inclination towards the formation of hydrogen bonds within the polymer matrix, consequently contributing to enhancements in TS. Furthermore, the inclusion of NFC into the PLA/PBS matrix may form a rigid fibrillar network; meanwhile, TCNP1.0 provides interfacial interactions. Ferreira *et al.* (2023) reported that the addition of nanocellulose and nano-encapsulated EO acts as a reinforcing phase, improving matrix cohesion and stiffness. Therefore, these combined effects restrict polymer mobility and enhance stress transfer (Omran *et al.* 2021), leading to enhanced TS. The improvement in mechanical properties after incorporation of 5 wt% of TCNP1.0 is particularly important for active packaging applications, whereby higher EaB reduces the risk of brittle fractures under tensile stress and improves resistance during the handling process.

The addition of 7 wt% TCNP1.0 reduced the EaB value of PLA/PBS and PLA/PBS/NFC films. This suggests that TCNP1.0 acts as a plasticizer, possibly due to the oil exudation from the capsule. Additionally, during the test load application, the capsules may have been pulled and deformed, affecting the diffusion of oil through the polymeric matrix (Ghani *et al.* 2018). Meanwhile, the addition of free thymol displays a significant reduction in TS with high EaB values, indicating excessive plasticization effects. Although high values of EaB were obtained, lower TS may limit the ability of these films to withstand mechanical stress. Moreover, at high amounts, thymol may have a strong phenolic, herbal, and pungent aroma (Kowalczyk *et al.* 2020). For example, strawberries have a delicate flavour profile, but excessive thymol may potentially overpower these natural aromas. However, the addition of CNP reduced the mechanical properties of films; higher content may promote more agglomeration of nanofillers and nanoparticles, which further reduces the TS.

Quantification of Thymol Content

The 95% ethanol was selected for this analysis due to the high solubility of thymol in ethanol and to ensure the diffusion of thymol. The amount of remaining thymol in films after 48 h is shown in Table 2. The results suggest that 3 and 5 wt% of TCNP exhibited a higher percentage remaining in PLA/PBS and PLA/PBS/NFC films than pure thymol. A low concentration of pure thymol incorporated into films may lose its active agents during the solvent casting drying process. Meanwhile, a low amount of TCNP remained in films with a high percentage, which might be due to the TCNP being well dispersed in films. The 5 wt% percentage of TCNP had the highest percentage in PLA/PBS, and PLA/PBS/NFC films with 41 and 48%. This can be explained by the addition of 5 wt% of TCNP, which fosters a strong hydrogen bond network with polymer chains, which can be observed by the mechanical property findings (Li *et al.* 2021).

In comparison, at a higher concentration (7 wt%), pure thymol demonstrated a higher percentage than TCNP. This is mainly due to the aggregation of nanoparticles that occurs in the polymer matrix. Aggregate particles have less surface area, which results in weaker interfacial interaction with the polymer, which increases the thymol leakage or volatilization (Biswal *et al.* 2019). Thus, a high concentration gradient due to low affinity between TCNP and the polymer chain drives the loss of thymol. The PLA/PBS/NFC films incorporated with pure thymol and TCNP possess a high percentage remaining in the films. This may be attributed to thymol being a non-polar compound, showing high solubility in ethanol, and may be related to the extent of swelling of the PLA/PBS matrix. The previous study, Saez-Orviz *et al.* (2020), who prepared thymol encapsulated in PLA nanoparticles and incorporated in gelatine films, observed only a small percentage of thymol remained in the films because most of the pure thymol evaporated during drying due to its high volatility and poor binding with gelatine, while thymol encapsulated in PLA nanoparticles showed slightly better retention.

Taking into account the remaining amounts and mechanical properties, 5 wt% can be considered as optimal loading for the comparison with pure thymol and CNP in the following analysis.

Table 2. Amounts of Thymol Remaining After 48 h in 95% Ethanol at 45 °C

Films	Concentration (wt%)	Thymol Remained in Films (%)	Films	Concentration (wt%)	Thymol Remained in Films (%)
PLA/PBS/T	3	10.8	PLA/PBS/NFC/T	3	31.9
	5	25.6		5	36.7
	7	31.2		7	46.6
PLA/PBS/TCNP1.0	3	22.7	PLA/PBS/NFC/TCNP1.0	3	40.6
	5	41.2		5	48.2
	7	25.7		7	36.7

FTIR of Selected Films

The molecular interactions of 5 wt% of CNP, pure thymol, and TCNP1.0 in PLA/PBS and PLA/PBS/NFC films were recorded by FTIR analysis and are shown in Fig. 6A. The major characteristic bands in neat PLA/PBS, including peaks at 1760 cm^{-1} are linked to the carbonyl group of lactides of PLA, the peak at 1454 cm^{-1} corresponds to the bending vibration of CH_3 of PLA (Mohamad *et al.* 2022), the peak ranging from 1300 to 1500 cm^{-1} represents C-O stretching of the ester group, and the peak at 1000 to 1250 cm^{-1} (C=O stretching of carbonyl group) of PBS (Vorawongsagul *et al.* 2021). The PLA/PBS/NFC films exhibited the major bands at 2976 cm^{-1} (symmetric C–H vibrations of NFC), and 1079 and 756 cm−1 peaks were predominantly linked to the stretching vibration of C–O-C and C–OH and the out-of-plane bending mode of NFC, respectively, in Fig. 6B (Mao *et al.* 2019).

The incorporation of pure thymol resulted in additional absorbance bands at 3494 and 3475 cm^{-1} for PLA/PBS, and PLA/PBS/NFC films, which was likely due to the stretching vibration of hydroxyl groups (Di Matteo *et al.* 2025). Additionally, the spectrum showed the phenolic ring of thymol at 1458 cm^{-1}, and phenolic C-O stretching located at 1215 cm^{-1}. A peak at 869 cm^{-1} is related to an out-of-plane aromatic C-H stretching vibration. Spectra films with CNP have an observable peak at 1189 and 1197 cm^{-1} for PLA/PBS, and PLA/PBS/NFC films, respectively, related to the amino group of chitosan present in the capsule of TCNP (Gomathi *et al.* 2017).

After the addition of TCNP1.0, slight changes in the FTIR spectrum were observed. The most important change was the changes in the intensity of peaks and the shift in wavenumber. The peaks of PLA/PBS and PLA/PBS/NFC films at 1760 and 1763 cm^{-1} were shifted to the lower wavenumber, appearing at 1748 and 1746 cm^{-1}, suggesting that intermolecular interactions occurred (Ghaderi-Ghahfarokhi *et al.* 2016). Moreover, the emergence of new peaks at 3744 and 3746 cm^{-1} was observed to be related to the OH and NH groups stretching of chitosan, which was also observed in spectra films incorporated with TCNP. The intensity of the peak increased to 1094 and 1089 cm^{-1} in PLA/PBS and

PLA/PBS/NFC films incorporated with TCNP1.0, which was attributed to the presence of thymol, and confirms the electrostatic interactions within the matrix network.

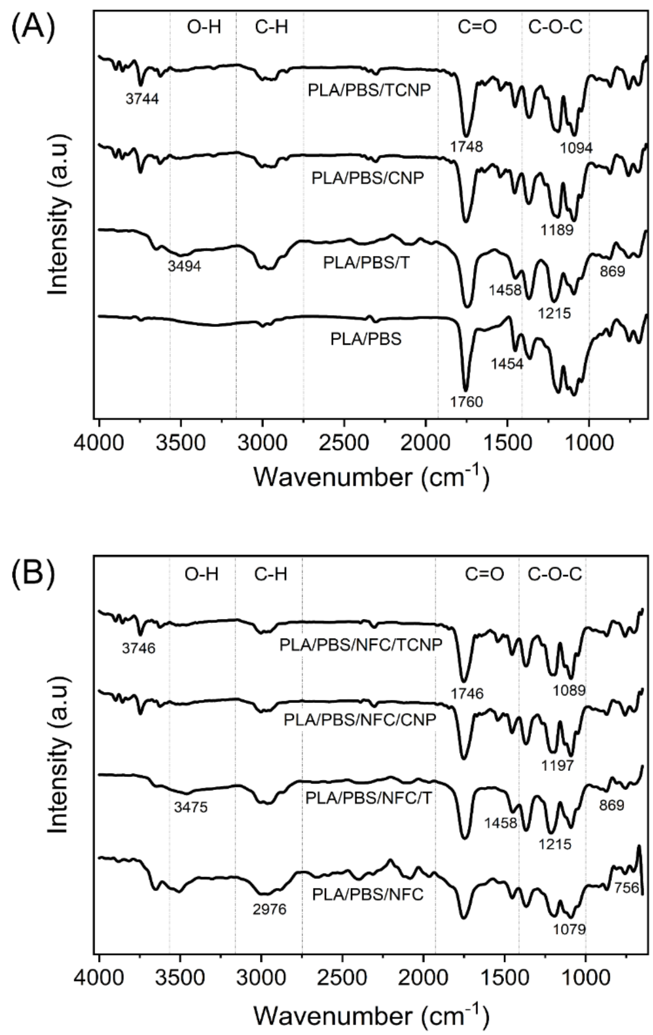

Fig. 6. FTIR spectra of active (A) PLA/PBS and (B) PLA/PBS/NFC incorporated with 5 wt% of pure thymol, CNP, and TCNP1.0

Thermal Stability of Selected Films

The thermal profile of PLA/PBS and PLA/PBS/NFC incorporated with 5 wt% pure thymol, CNP, and TCNP1.0 is demonstrated in Fig. 7. The TGA thermogram of PLA/PBS and PLA/PBS/CNP film exhibited two-step weight loss. The first step, occurring at T = 300 to 400 °C, was due to the degradation of the PLA polymer. The second step occurred within the temperature range of 400 to 420°C, corresponding to the degradation of PBS polymer (Vorawongsagul *et al.* 2021), which involves the random breakdown of the ester linkages through β-CH hydrogen transfer, forming carboxylic end groups and vinyl groups (Arman Alim *et al.* 2023). In contrast, PLA/PBS/T and PLA/PBS/TCNP exhibited a three-step thermal degradation event. The initial stage occurred below 200 °C, with an initial degradation temperature of T_i = 96 °C for PLA/PBS/T and T_i = 150 °C for PLA/PBS/TCNP. The inclusion of pure thymol in films is widely recognized to primarily result in the volatilization of thymol during the film's casting process, as evidenced in Fig.

7A. This stage suggests that the encapsulation process, with the presence of chitosan-STPP cross-links, could enhance the thermal stability of PLA/PBS films.

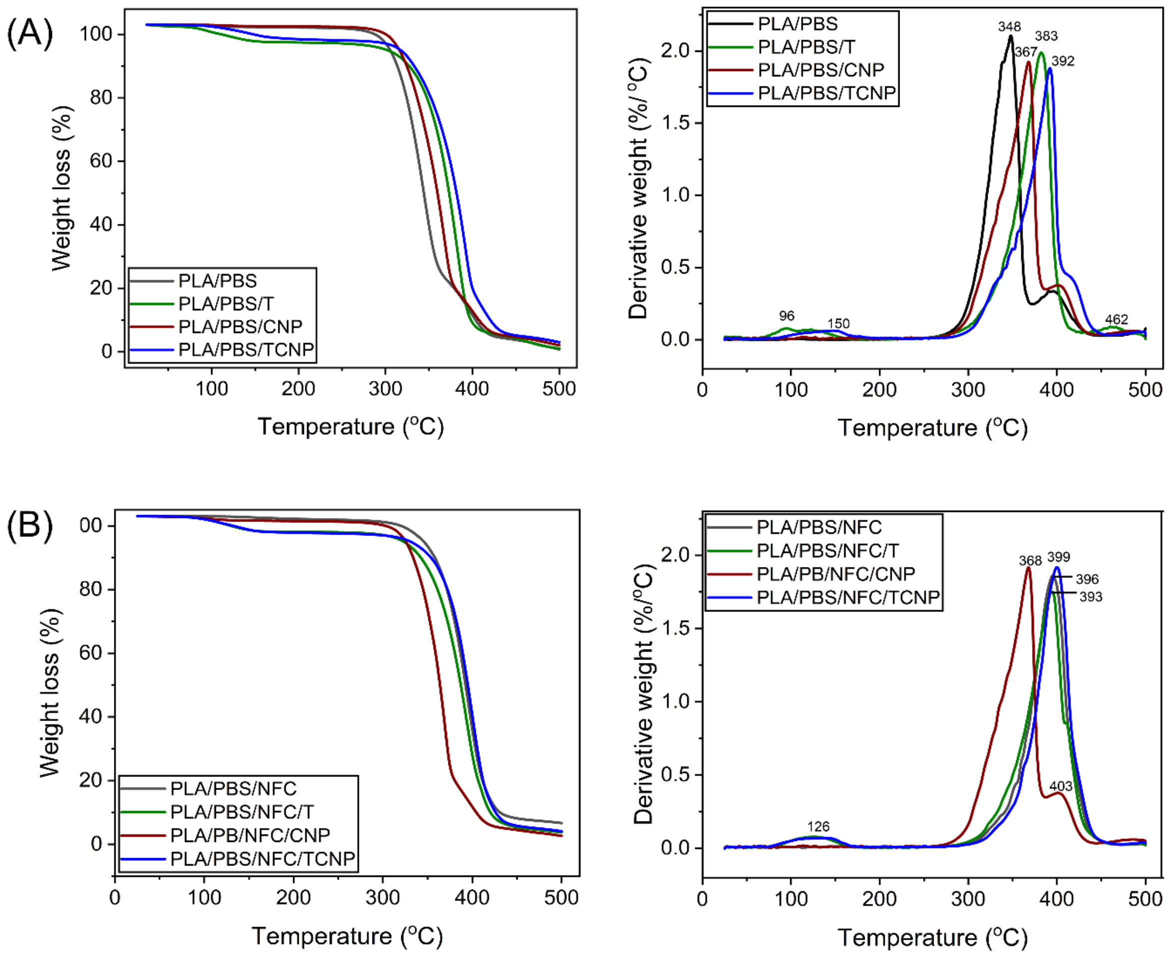

Fig. 7. TGA and DTG profile of (A) PLA/PBS, and (B) PLA/PBS/NFC films incorporated with 5 wt% of pure thymol, CNP, and TCNP1.0

In the second step, the maximum degradation temperature (T_{max}) was observed at a range of 340 to 400 °C, which can be attributed to the thermal degradation of the PLA polymer chain. Comparing the PLA/PBS/T (T_{max} = 383 °C) with that of PLA/PBS/TCNP (T_{max} = 383 °C) reflects an enhancement in thermal stability. However, in the third thermal event, the shoulder peak was not detectable for the PLA/PBS/T and PLA/PBS/TCNP. This may be attributed to the plasticizing effects and possible interaction between pure thymol and TCNP, which could restrict their molecular mobility when the PBS is in a minor phase (Kennouche *et al.* 2016). Król-Morkisz and Pielichowska (2019) stated that the formation of bonds containing structures in the primary chains makes polymers resistant to high temperatures.

The PLA/PBS/NFC films exhibited three-step weight loss with enhanced T_{max} (368 °C) compared with PLA/PBS films (T_{max} 348 °C) in Fig. 7B. Comparable results were reported by Ferreira *et al.* (2023), who demonstrated that adding cinnamon EO and Ho wood-loaded chitosan nano-capsules increased the T_{max} of PBAT/nanocellulose films. This outcome could be attributed to the nano-capsule TCNP facilitating the molecular interaction within the PLA/PBS/NFC matrix. Moreover, PLA/PBS/NFC/T was prominently noticed at 383 °C; however, upon incorporation of TCNP1.0, the T_{max} was increased to 392 °C. Encapsulated thymol decomposed at a higher temperature than pure thymol in PLA/PBS/NFC films, which was caused by the strong bonding forces of TCNP1.0 and NFC may require more energy to decompose, leading to a higher degradation temperature. These results suggested that the PLA/PBS/NFC/TCNP film could withstand high temperatures. Thus, it could be used as a packaging material under heat treatments such as pasteurization or sterilization (Soltanzadeh *et al.* 2021).

Properties for Food Packaging Applications

This section focused on the comparison between the optimized formulation of TCNP1.0 (5 wt%) and CNP, as well as pure thymol, in terms of water barrier, light transmittance, liquid culture, and toxicity assay. Among the three concentrations, the PLA/PBS and PLA/PBS/NFC films containing 5 wt% exhibited the most balanced mechanical performance, with significant increases in TS and EaB. Quantification by the UV-Vis spectrometer was further supported by containing the highest percentage remaining in films after 48 h. Moreover, FTIR and thermal analysis of PLA/PBS and PLA/PBS/NFC films incorporated with 5 wt% of TCNP1.0 showed intermolecular interaction and high thermal stability. Therefore, the concentration (5 wt%) was selected as the optimized formulation for further food packaging application testing when compared with CNP and pure thymol.

Barrier Properties

The WVP represents a critical characteristic of packaging materials, essential for minimizing moisture transfer from the external environment to the contained food substances or packaged goods. It is crucial to maintain the lowest possible WVP value to ensure the preservation of food freshness. The WVP is affected by several factors, including the polymer chain structure, hydrophobic properties, and the concentration of additives (Gasti *et al.* 2022). The WVP values of active films are depicted in Fig. 8. Neat PLA/PBS and PLA/PBS/NFC films exhibited WVP values at 5.35 and 5.67 × 10 to 12 g/Pa · h · m.

The incorporation of 5 wt% of TCNP1.0 was found to reduce WVP values of PLA/PBS, and PLA/PBS/NFC films by 7.8% and 10.1%, respectively. The reduction in WVP value was attributed to the good compatibility of TCNP and the polymer matrix, as revealed in the FTIR result above. The inclusion of TCNP1.0 created a dense torturous path for water diffusion due to the restricted mobility of the polymer chain (Camani *et al.* 2021), which leads to a lower WVP value. In comparison, PLA/PBS/TCNP has a lower WVP value compared with PLA/PBS/NFC/TCNP. This can be due to the hydrophilic nature of NFC, which increases the solubility and diffusivity of water in the polymer matrix (de Medeiros *et al.* 2019).

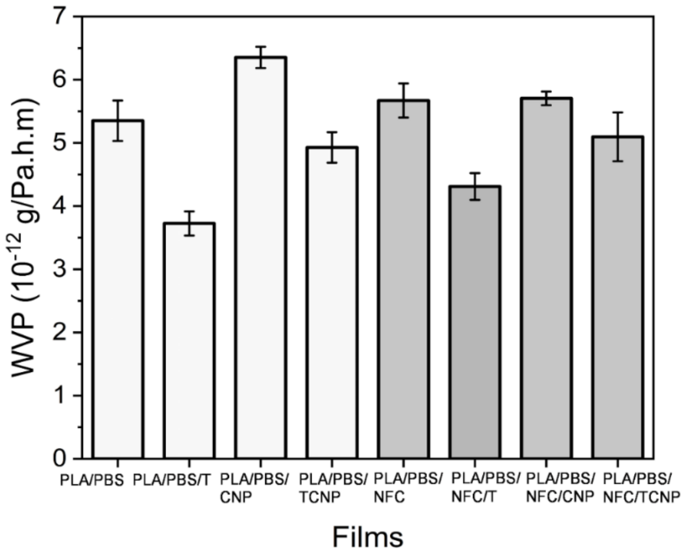

Fig. 8. WVP of PLA/PBS and PLA/PBS/NFC films incorporated with 5 wt% of pure thymol, CNP, and TCNP

As expected, the inclusion of pure thymol resulted in decreasing WVP values of PLA/PBS and PLA/PBS/NFC films. Enhancing the hydrophobicity of PLA/PBS matrices was observed with the presence of 5 wt% of pure thymol. Similarly, Laorenza *et al.* (2021), incorporated EO in the PLA/PBAT matrix, stating that EO yields a reduction in the crystallinity of matrices and has a notable impact on WVP properties. Moreover, the incorporation of CNP in PLA/PBS and PLA/PBS/NFC matrix increased the WVP value. It can be suggested that CNP addition affects the hydrophilicity of films, consequently impeding the creation of a convoluted path within the matrices.

Light Transmittance

The transparency of active films is the indicator that affects general appearances and consumer acceptance. Light transmittance properties of bio-nanocomposite films were determined over wavelengths ranging from 350 to 800 nm, as shown in Fig. 9. PLA/PBS/T showed a weak UV light barrier property, directly affecting food preservation. Encouragingly, the transmittance decreased with CNP and TCNP1.0 incorporation, indicating the films had strong UV barrier performance. The inclusion of pure thymol increased the transparency of PLA/PBS and PLA/PBS/NFC films due to the aromatic ring group present in polyphenolic substances. Thymol has a strong UV absorption property (Keawchaoon and Yoksan 2011).

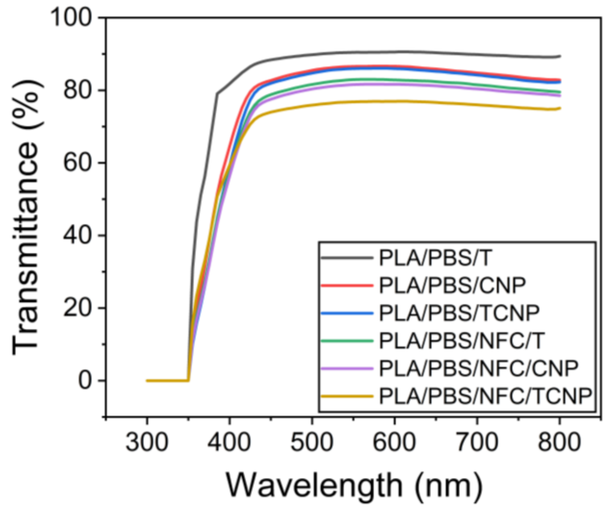

Fig. 9. Light transmittance (%T) of active PLA/PBS and PLA/PBS/NFC incorporated with pure thymol, CNP, and TCNP1.0

Regarding the transparency of nanocomposite films, the incorporation of CNP and TCNP1.0 in PLA/PBS/NFC films displayed a low transmittance value, exhibiting 81.6% and 76.9%, respectively. The inclusion of NFC resulted in a minor reduction in PLA/PBS film's transparency, which could be ascribed to the nanofiller's function in the prevention of light transmission, thus offering potential advantages in terms of UV light prevention and protection (Talebi *et al.* 2018). The incorporation of CNP into PLA/PBS/NFC films results in the lowest transparency to visible light, as the aggregation of CNP fills the void in the polymer matrix, blocking visible light, which is in good agreement with Garavand *et al.* (2022). Compared to pure thymol, nano-sized TCNP1.0 scatters shorter wavelengths, compromising less on the film's transparency while providing superior UV barrier characteristics. Consumers may prefer high transparency, but lower transparency can act as a barrier to light, protecting food from degradation (Costa *et al.* 2021).

Assessment of Antimicrobial Activity

Antibacterial assay is the most important factor for active films, since it indicates the safety of foods, which is likely due to the microbes in food (Ge *et al.* 2022). The antibacterial effects of the films were studied against *S. aureus* and *E. coli*. The liquid culture assay was used to evaluate the antibacterial effects, in which bacterial growth inhibition was determined by viable cell counts (log CFU/mL) after 24 h incubation. The lower value of bacterial counts reflects stronger inhibitory effects, which indicates higher antibacterial effects, as depicted in Fig. 10.

The incorporation of 5 wt% of TCNP1.0 in PLA/PBS and PLA/PBS/NFC films showed a stronger antibacterial activity for *S. aureus* compared with *E. coli*, as evidenced by the lower bacterial count (log CFU/mL). This may be due to the synergic effects of CNP and thymol, which lets ions in CNPs to interact with the cell membrane of bacteria, thus allowing the slow release of thymol to inhibit the growth of bacteria. Renowned for its potent antibacterial capabilities, chitosan is believed to be effective due to its polycationic nature (Roy *et al.* 2024). This can be attributed to the affinity of chitosan's positively charged amine groups with the negatively charged surface of bacterial membranes, which induces alterations in cellular permeability that lead to cell lysis, as shown in Fig. 11. Feyzioglu *et al.* (2016) reported an enhanced antibacterial activity of summer savory

(*Satureja hortensis* L.) EO nano-encapsulated in CNP. A study by Oluoch *et al.* (2021) further supports the findings, which reported enhanced antibacterial effects of chitosan encapsulated with thymol and eugenol EO against *Ralstonia solanacearum*.

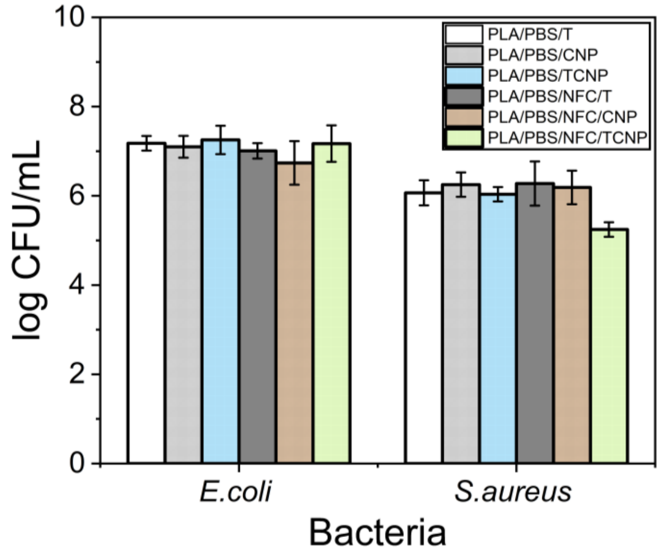

Fig. 10. Antimicrobial activity of PLA/PBS and PLA/PBS/NFC-films with the incorporation of pure thymol, CNP, and TCNP1.0 against *S. aureus* and *E. coli* after 24 h

The lower antibacterial effects of TCNP1.0 on *E. coli* compared with *S. aureus* may be due to the composition and structure of Gram-negative bacteria. Kalajahi *et al.* (2024) stated that Gram- negative bacteria are made up of an outer membrane that consists of phospholipids, lipopolysaccharides, and a thin peptidoglycan layer near the cytoplasmic membrane, which may limit the penetration of thymol. But, as observed, the addition of 5 wt% of pure thymol resulted in slightly higher inhibition compared with TCNP1.0 for *E. coli* in PLA/PBS and PLA/PBS/NFC films. This phenomenon may occur due to the reduction of bioavailability of active compounds due to the encapsulation process. Silva *et al.* (2025) stated that encapsulation *via* the IG techniques is a way to preserve antibacterial properties in the long term, which may result in TCNP1.0 not reaching a sufficient concentration that can effectively disrupt the outer membrane of *E. coli.* Meanwhile, the pure thymol was freely available, allowing direct interaction with microbial cells to suppress the bacterial growth. Thymol is a well-known active compound for its intense antibacterial action against many bacteria. This property is believed to be due to thymol-induced perforation in the bacterial cell's plasma membrane. As a result, thymol causes a decrease in intracellular ATP by inhibiting the electron transport system, which destroys the cell membrane (Mittal *et al.* 2019). The cell death occurred after massive ion leakage, as shown in Fig. 11.

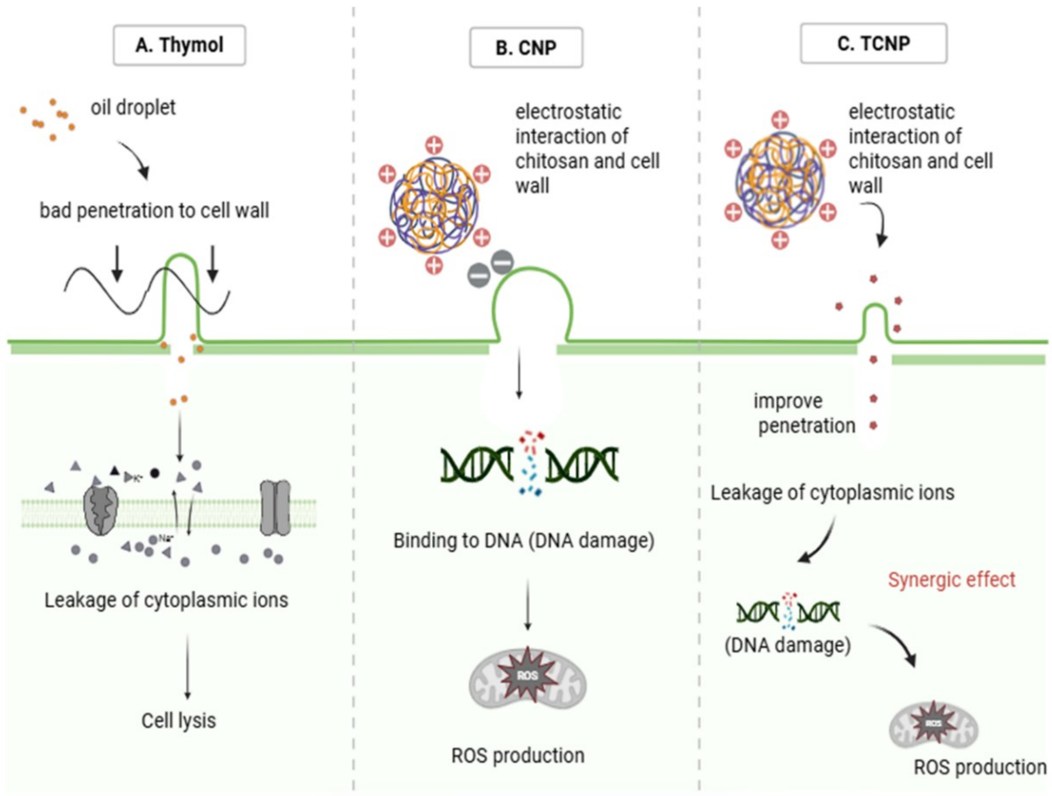

Fig. 11. Proposed antibacterial mechanisms of the synergistic effect of pure thymol, CNP, and TCNP1.0

Moreover, the reduction of bacteria of pure thymol and TCNP1.0 for *E. coli* can be observed to be slightly lower than CNP in PLA/PBS/NFC films. This may be due to the electrostatic interaction of positively charged protonated amino groups with negatively charged lipopolysaccharide (LPS) of *E. coli*. However, for TCNP1.0, when thymol is encapsulated in CNP, the hydrogen bonds that form between CNP and thymol may reduce the availability of free functional groups of CNP that can contribute to the electrostatic interaction. Besides, the core region of LPS in *E. coli* may act as a barrier against hydrophobic compounds, such as thymol, and restrict their penetration (Wang, J. *et al.* 2021). Therefore, it may cause delayed release and limit the penetration of thymol. On the other hand, *S. aureus* bacteria have a thick but porous peptidoglycan layer (Pasquina-Lemonche *et al.* 2020) that can allow easier penetration of TCNP1.0 to damage the membrane layer and cause cell death.

Toxicity Assay

Cellular cytotoxicity is characterized based on biochemical responses that evaluate the metabolic functionality of viable cells. Assessment of cell viability was a prevalent method employed to predict the potential toxicity of substances by gauging the survival rates of cells. Ensuring the safety of nanomaterials (TCNP1.0) nano-capsules within bio-nanocomposite films for utilization in the food packaging sector is of paramount importance. The present literature offers limited insight regarding the cytotoxic activity of active films. Therefore, an MTT assay was executed to demonstrate that 3T3 fibroblast cell lines maintain a standard metabolic rate and proliferation in the presence of the highest loading (7 wt%) of TCNP in PLA/PBS, alongside PLA/PBS/NFC films, with the corresponding data depicted in Fig. 12. Through the experimental procedure, it was determined that cell viability remained notably above 80% after 48 h of direct interaction between all films and cells ($p < 0.05$). The PLA/PBS and PLA/PBS/NFC films incorporated with CNP exhibited a cell viability reduction of around 16 and 12%, respectively. The addition of CNP did not present relevant cell toxicity even at higher concentrations. Kumar *et al.* (2015) found no significant decrease in cell mass of 3T3 fibroblasts when in contact with the chitosan NP. Meanwhile, as for the incorporation of TCNP1.0, the viability cells were found to be 82 ± 3.44 and 85 ± 2.01%, respectively. These results confirmed that the developed PLA/PBS/NFC/TCNP films had lower apparent cytotoxicity against the 3T3 fibroblast cells due to the presence of nontoxic chitosan and lower amounts of NFC. The study showed that the polyhydroxybutyrate (PHB)-based graphene nanocomposites, prepared by solvent casting methods in chloroform solutions, present 79% viability of cells (Manikandan *et al.* 2020). Therefore, it is reasonably safe to implement it in films in the concentration range of 3 to 7 wt% of TCNP1.0. As per the biological appraisal outlined in medical devices – Part 5: tests for *in vitro* cytocompatibility (ISO 10993-5 2009) – the material's cell viability ought to exceed 70% to be classified as biocompatible (Socrates *et al.* 2019). Hence, the bio-nanocomposite films with the incorporation of TCNP1.0 are considered suitable for food packaging applications.

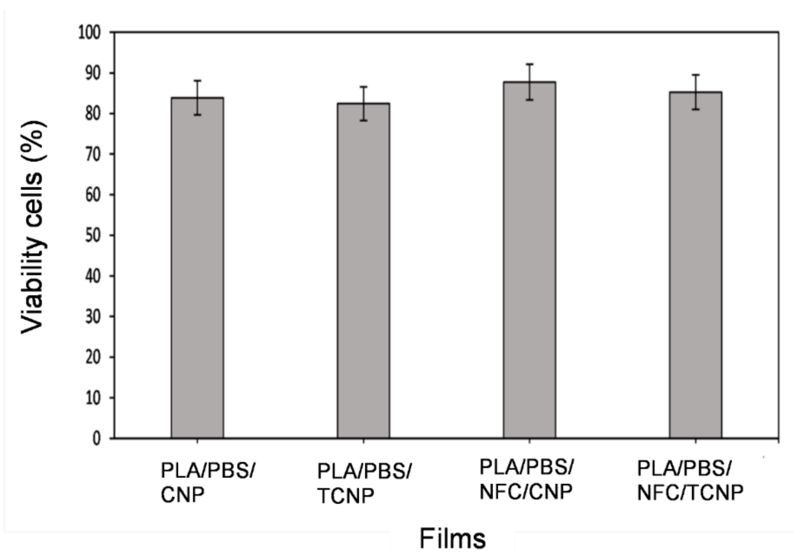

Fig. 12. Toxicity assay of PLA/PBS and PLA/PBS/NFC films incorporated with pure thymol and TCNP

Release Test

The release test is important for evaluation of packaging performance for the preservation of food. The release test of pure and encapsulated thymol from PLA/PBS and PLA/PBS/NFC films was carried out to evaluate the controlled release of TCNP1.0 resulting from encapsulation by IG methods. As shown in Fig. 13, the PLA/PBS/T and PLA/PBS/NFC/T exhibited a burst of release during the first 10 h, then it released slowly until reaching equilibrium. This could be due to the immediate diffusion of pure thymol from the film's surface, which diffuses rapidly to the food simulant (Sharma *et al.* 2023). By contrast, for PLA/PBS and PLA/PBS/NFC films containing TCNP1.0, the release was increased steadily within 48 h, indicating that thymol was confined in the chitosan matrix and needed more time to reach the equilibrium state. In food packaging applications, rapid release can quickly inhibit the growth of microorganisms; meanwhile, slow release can provide long-term protection of food (Li, B. *et al.* 2025).

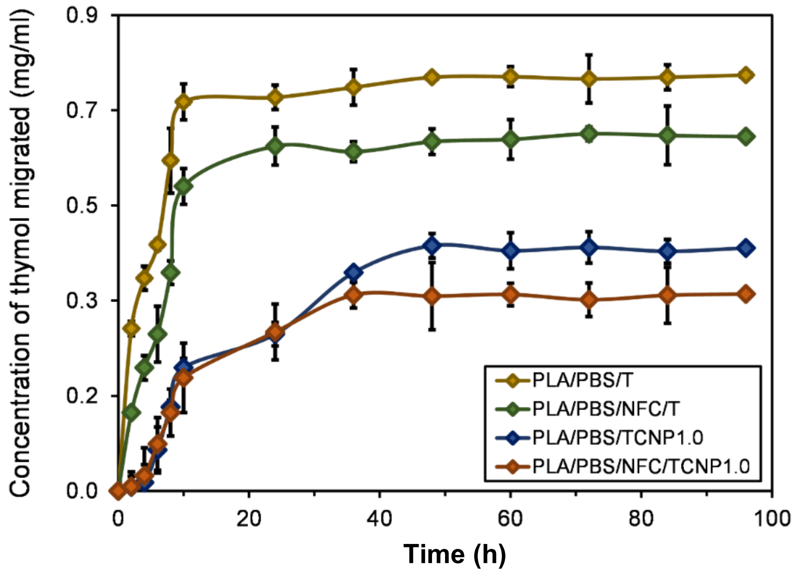

Fig. 13. Release test of PLA/PBS and PLA/PBS/NFC films containing pure thymol and enCAPSulate (TCNP1.0) in 95% ethanol at 45 ºC

As a preservation strategy, the films need to have a sustained and controlled release. For instance, where the release rate surpasses the rate of microbial proliferation, the efficacy of antimicrobial properties will be depleted before the end of the product's shelf-life (Fadiji *et al*. 2023), consequently facilitating microbial proliferation within packaged food products. Conversely, if the release rate is excessively slow, microbial growth will accelerate before the release of the EOs. In the 95% ethanol at 45 ºC, the equilibrium stages were extended to 96 hours. Similarly, Yu *et al.* (2023) observed low and sustained release rate patterns in hydroxypropyl methylcellulose/hydroxypropyl starch films incorporating nano-encapsulated cinnamon EO in 95% food simulants for 96 hours. Moreover, at 45 ºC, the release rate was fast due to the increased mobility of PLA-based film chains as the temperature approached the glass transition temperature of PLA (55-65 ºC) (De Luca *et al.* 2023). Rojas *et al.* (2021) reported that as an active PLA film's glass transition temperature, the polymer chains become more mobile, facilitating diffusion through amorphous regions.

A previous study by Hajirostamloo *et al.* (2023) showed that free cardamom oil gave a rapid and high burst release, while microencapsulated cardamom oil followed a slow and controlled release pattern over time in soy protein isolate films. Additionally, Lanciu Dorofte *et al*. (2023) reported that encapsulation of thyme EO in the β-CD inclusion complexes (ICs) exhibits a slow, uniform diffusion and noted that a higher release rate at 95% ethanol in whey protein edible films. This is because thymol is a hydrophobic compound that exhibits high solubility in alcohols, including ethanol (Kowalczyk *et al.* 2020). Moreover, a higher release rate was observed for PLA/PBS films compared with PLA/PBS/NFC films. When it comes in contact with food simulants, the rate of swelling depends on the polarity and affinity of the simulant and polymer matrix material. Harper *et al.* (2022) stated that high affinity between food simulants and polymer matrix will lead to the absorption of solvents, causing greater swelling, which can contribute to enlarging the gap between molecules and migration of small particles. Meanwhile, low affinity induces less swelling, and the additives will remain in the food matrix. Ethanol, particularly 95%, can act as a strong plasticizer for PLA and PBS biopolymer which can penetrate and interact with polymer chains and induce swelling effects.

Appearance Change and Weight Loss of Fresh-cut Strawberries

Strawberries are a ubiquitous fruit with a distinct taste, appearance, and nutrient benefits. Strawberries have a relatively short shelf life because of physiological deterioration, susceptibility to microbial contamination, and their delicate tissue structure. To evaluate the practical feasibility of the prepared films in food preservation, fresh-cut strawberries were packaged using the selected films. Strawberry colour and appearance are direct indicators of its quality and freshness. Most of the strawberries kept their fresh appearance, exhibited a red colour, and showed no signs of degeneration after 5 days of storage at 4 °C in Fig. 14.

Meanwhile, the weight loss of fresh-cut strawberries wrapped with PLA/PBS/TCNP1.0 and PLA/PBS/NFC/TCNP1.0 was 11.31% and 14.65%, respectively, which were less than PLA/PBS/NFC/T, which was also attributed to the thymol release. During the diffusion of moisture through the film, thymol was probably released into the packaging and prevented the appearance of fungi due to its bioactive action. The lower weight loss of the strawberry indicated that the films play an important role as a water vapour barrier between the strawberry and the environment throughout the storage period (Cai *et al.* 2020). Without the barrier, it is easy for the water in strawberries to evaporate into the surroundings. Nonetheless, the strawberry wrapped with PLA/PBS/T showed a high weight loss (44.8%), which is attributed to the reduced amount of water caused by the respiration and transpiration process throughout the storage. Moreover, Pastor *et al.* (2011) stated that the acceleration of weight loss, which can be attributed to an increase in the fruit's metabolic activity, associated with tissue senescence over long storage time, is slowed down after wrapping application. The incorporation of TCNP1.0 showed lower weight loss and prolonged shelf-life, indicating that the fruits were not affected by any deterioration form, being acceptable for consumption.

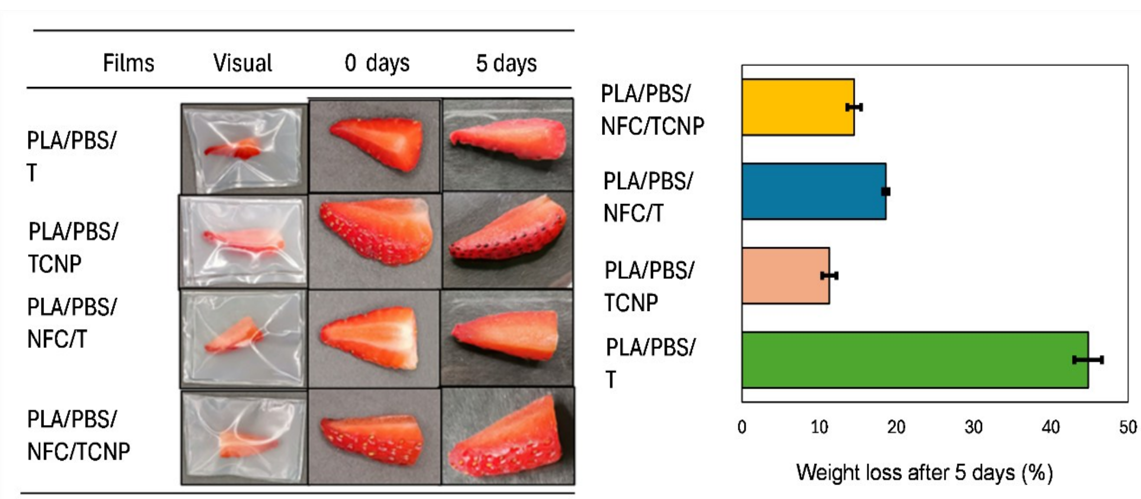

Fig. 14. Visual appearance and weight loss of fresh-cut strawberries after 5 days of storage

CONCLUSIONS

1. The poly(lactic acid)/poly(butylene succinate) (PLA/PBS) and the corresponding nanofibrillated cellulose (PLA/PBS/NFC)-based functional films were fabricated *via* solvent-casting by incorporating the different concentrations of thymol-loaded chitosan phosphate nanoparticle (TCNP) for active food packaging applications.
2. The presence of TCNP in PLA/PBS and PLA/PBS/NFC improved mechanical properties, particularly tensile strength (TS), and tensile modulus (TM), with minimal impact on the thermal stability of the film, which is attributed to the reinforcing effects of TCNP. Furthermore, the homogeneous dispersion and favorable compatibility of the PLA/PBS/NFC/TCNP films played a crucial role in enhancing the mechanical strength of the final films.
3. The Fourier transform infrared (FTIR) spectra confirmed chemical interactions between PLA/PBS/NFC and thymol essential oil (EO) nano-capsules in the polymer matrix. Simultaneously, the improvements of water barrier properties in PLA/PBS/NFC films incorporating TCNP exhibited good compatibility due to the bonding capabilities between the matrix and the reinforcing phase.
4. The developed films exhibit bacteriostatic activity against food-borne pathogens. Films containing TCNP1.0 generally show stronger inhibition of *S. aureus* bacteria due to the synergistic effects, whereas films with CNP were more effective against *E. coli* bacteria, which were highly dependent on the structure of the bacteria and the release of thymol.
5. These findings can provide insight into the potential use of TCNP1.0 in bio-based packaging materials. However, the additional information on the safety of nanomaterials and the release kinetics of TCNP1.0 would further strengthen the packaging applications.

Conflicts of Interest

The authors declare no conflict of interest.

Acknowledgments

The authors would like to thank the Institute of Tropical Forestry and Forest Products (INTROP), Universiti Putra Malaysia, for the research facilities and support. This study was financially supported by Universiti Putra Malaysia under the Geran Putra Berimpak (GPB/2024/9810100).

REFERENCES CITED

Abdullah, T., Saeed, U., Memic, A., Gauthaman, K., Hussain, M. A., and Al-Turaif, H. (2019). "Electrospun cellulose nano fibril reinforced PLA/PBS composite scaffold for vascular tissue engineering," *Journal of Polymer Research* 26, article 110. https://doi.org/10.1007/s10965-019-1772-y

Abushal, S. A., Elhendy, H. A., and Soliman, T. N. (2025). "Nanoencapsulation of *Thyme oleoresin*: A novel strategy to enhance bioactive ingredients' bioaccessibility in functional UF-Labneh and prolong shelf life," *Journal of Future Foods* (in press). https://doi.org/10.1016/j.jfutfo.2025.03.013.

Alehosseini, E., Shahiri Tabarestani, H., Kharazmi, M. S., and Jafari, S. M. (2022). "Physicochemical, thermal, and morphological properties of chitosan nanoparticles produced by ionic gelation," *Foods* 11(23), article 3841. https://doi.org/10.3390/foods11233841

Alizadeh-Sani, M., Moghaddas Kia, E., Ghasempour, Z., and Ehsani, A. (2021). "Preparation of active nanocomposite film consisting of sodium caseinate, ZnO nanoparticles and rosemary essential oil for food packaging applications," *Journal of Polymers and the Environment* 29(2), 588-598. https://doi.org/10.1007/s10924-020-01906-5

Almasi, L., Radi, M., Amiri, S., and McClements, D. J. (2021). "Fabrication and characterization of antimicrobial biopolymer films containing essential oil-loaded microemulsions or nanoemulsions," *Food Hydrocolloids* 117, article 106733. https://doi.org/10.1016/j.foodhyd.2021.106733

Anand, M., Sathyapriya, P., Maruthupandy, M., and Beevi, A. H. (2018). "Synthesis of chitosan nanoparticles by TPP and their potential mosquito larvicidal application," *Frontiers in Laboratory Medicine* 2(2), 72-78. https://doi.org/10.1016/j.flm.2018.07.003

Angane, M., Swift, S., Huang, K., Butts, C. A., and Quek, S. Y. (2022). "Essential oils and their major components: an updated review on antimicrobial activities, mechanism of action and their potential application in the food industry," *Foods* 11(3), article 464. https://doi.org/10.3390/foods11030464

Assadpour, E., and Mahdi Jafari, S. (2019). "A systematic review on nanoencapsulation of food bioactive ingredients and nutraceuticals by various nanocarriers," *Critical Reviews in Food Science and Nutrition* 59(19), 3129-3151. https://doi.org/10.1080/10408398.2018.1484687

Barrera-Ruiz, D. G., Cuestas-Rosas, G. C., Sánchez-Mariñez, R. I., Álvarez-Ainza, M. L., Moreno-Ibarra, G. M., López-Meneses, A. K., and Cortez-Rocha, M. O. (2020). "Antibacterial activity of essential oils encapsulated in chitosan nanoparticles," *Food Science & Technology* 40, 568-573. https://doi.org/10.1590/fst.34519

Basavegowda, N., and Baek, K. H. (2021). "Advances in functional biopolymer-based nanocomposites for active food packaging applications," *Polymers* 13(23), article 4198. https://doi.org/10.3390/polym13234198

Biswal, A. K., Vashisht, I., Khan, A., Sharma, S., and Saha, S. (2019). "Synthesis, characterization and antibacterial activity of thymol-loaded polylactic acid microparticles entrapped with essential oils of varying viscosity," *Journal of Materials Science* 54(13), 9745-9758.

Boeira, C. P., Flores, D. C. B., dos Santos Alves, J., de Moura, M. R., Melo, P. T. S., Rolim, C. M. B., and da Rosa, C. S. (2022). "Effect of corn stigma extract on physical and antioxidant properties of biodegradable and edible gelatin and corn starch films," *International Journal of Biological Macromolecules* 208, 698-706. https://doi.org/10.1016/j.ijbiomac.2022.03.164

Bumbudsanpharoke, N., Wongphan, P., Promhuad, K., Leelaphiwat, P., and Harnkarnsujarit, N. (2022). "Morphology and permeability of bio-based poly (butylene adipate-co-terephthalate)(PBAT), poly (butylene succinate)(PBS) and linear low-density polyethylene (LLDPE) blend films control shelf-life of packaged bread," *Food Control* 132, article 108541. https://doi.org/10.1016/j.foodcont.2021.108541

Cai, C., Ma, R., Duan, M., Deng, Y., Liu, T., and Lu, D. (2020). "Effect of starch film containing thyme essential oil microcapsules on physicochemical activity of mango," *LWT-Food Science and Technology* 131, article 109700. https://doi.org/10.1016/j.lwt.2020.109700

Çakır, M. A., Icyer, N. C., and Tornuk, F. (2020). "Optimization of production parameters for fabrication of thymol-loaded chitosan nanoparticles," *International Journal of Biological Macromolecules* 151, 230-238. https://doi.org/10.1016/j.ijbiomac.2020.02.096

Camani, P. H., Souza, A. G., Barbosa, R. F. S., Zanini, N. C., Mulinari, D. R., and Rosa, D. S. (2021). "Comprehensive insight into surfactant modified-PBAT physico-chemical and biodegradability properties," *Chemosphere* 269(2021), article 128708. https://doi.org/10.1016/j.chemosphere.2020.128708

Chaudhari, A. K., Singh, V. K., Das, S., Prasad, J., Dwivedy, A. K., and Dubey, N. K. (2020). "Improvement of *in vitro* and *in situ* antifungal, AFB1 inhibitory and antioxidant activity of *Origanum majorana* L. essential oil through nanoemulsion and recommending as novel food preservative," *Food and Chemical Toxicology* 143, article 111536. https://doi.org/10.1016/j.fct.2020.111536

Chen, Q., Han, D., Qu, X., Zhang, W., Peng, Y., Li, S., and Gao, Z. (2025). "Self-enhanced multifunctional composite membranes based on metal-organic frameworks embedded with thymol nanoparticles for post-harvest preservation of fruits," *Food Hydrocolloids* 164, article 111208. https://doi.org/10.1016/j.foodhyd.2025.111208

Cheng, M., Yan, X., Cui, Y., Han, M., Wang, Y., Wang, J., Zhang, R., and Wang, X. (2022). "Characterization and release kinetics study of active packaging films based on modified starch and red cabbage anthocyanin extract," *Polymers* 14(6), article 1214. https://doi.org/10.3390/polym14061214

Corrado, I., Di Girolamo, R., Regalado-González, C., and Pezzella, C. (2022). "Polyhydroxyalkanoates-based nanoparticles as essential oil carriers," *Polymers* 14(1), article 166. https://doi.org/10.3390/polym14010166

Costa, S. M., Ferreira, D. P., Teixeira, P., Ballesteros, L. F., Teixeira, J. A., and Fangueiro, R. (2021). "Active natural-based films for food packaging applications: The combined effect of chitosan and nanocellulose," *International Journal of Biological Macromolecules* 177, 241-251. https://doi.org/10.1016/j.ijbiomac.2021.02.105

Dadashi, P., Bonsale, R., and Babaei, A. (2025). "Chitosan/ZnO nanohybrid as an efficacious compatibilizer for PLA/PBS blend suitable candidate for biodegradable packaging applications," *Scientific Reports* 15(1), article 41661. https://doi.org/10.1038/s41598-025-25596-y.

De Carvalho, F. G., Magalhães, T. C., Teixeira, N. M., Gondim, B. L. C., Carlo, H. L., Dos Santos, R. L., de Oliveiro, A. R., and Denadai, Â. M. L. (2019). "Synthesis and characterization of TPP/chitosan nanoparticles: Colloidal mechanism of reaction and antifungal effect on C. albicans biofilm formation," *Materials Science and Engineering: C* 104, article 109885. https://doi.org/10.1016/j.msec.2019.109885

de Dicastillo, C. L., Torres, A., Heras-Mozos, R., Guarda, A., and Galotto, M. J. (2025). "Thymol: Use in antimicrobial packaging," in: *Antimicrobial Food Packaging*, Academic Press, Cambridge, MA, USA, pp. 759-772. https://doi.org/10.1016/B978-0-323-90747-7.00049-1

De Luca, S., Milanese, D., Gallichi-Nottiani, D., Cavazza, A., and Sciancalepore, C. (2023). “Poly (lactic acid) and its blends for packaging application: A review,” *Clean Technologies* 5(4), 1304-1343. https://doi.org/10.3390/cleantechnol5040066

de Medeiros, J. A. S., Blick, A. P., Galindo, M. V., Alvim, I. D., Yamashita, F., Ueno, C. T., Shirai, M. A., Grosso, C. R. F., Corradini, E., and Sakanaka, L. S. (2019). “Incorporation of oregano essential oil microcapsules in starch-poly (butylene adipate co-terephthalate)(PBAT) films,” *Macromolecular Symposia* 383(1), article 1800052. https://doi.org/10.1002/masy.201800052

de Oliveira Filho, J. G., Miranda, M., Ferreira, M. D., and Plotto, A. (2021). “Nanoemulsions as edible coatings: A potential strategy for fresh fruits and vegetables preservation,” *Foods* 10(10), article 2438. https://doi.org/10.3390/foods10102438

Di Matteo, A., Stanzione, M., Orlo, E., Russo, C., Lavorgna, M., Buonocore, G. G., and Isidori, M. (2026). “Biodegradable films enriched with thymol and carvacrol with antioxidant and antibacterial properties to extend cheese shelf-life,” *Food Control* 179, article 111541. https://doi.org/10.1016/j.foodcont.2025.111541

dos Santos Paglione, I., Galindo, M. V., de Medeiros, J. A. S., Yamashita, F., Alvim, I. D., Grosso, C. R. F., and Shirai, M. A. (2019). “Comparative study of the properties of soy protein concentrate films containing free and encapsulated oregano essential oil,” *Food Packaging and Shelf Life*, 22, article 100419. https://doi.org/10.1016/j.fpsl.2019.100419

El-Aziz, A. R. M. A., Al-Othman, M. R., Mahmoud, M. A., Shehata, S. M., and Abdelazim, N. S. (2018). “Chitosan nanoparticles as a carrier for *Mentha longifolia* extract: Synthesis, characterization and antifungal activity,” *Current Science* 2018, 2116-2122.

European Commission. (2011). “Commission Regulation (EU) No 10/2011 of 14 January 2011 on plastic materials and articles intended to come into contact with food,” *Off. J. Eur. Union* 12, 1-89.

Esmaeili, A., and Asgari, A. (2015). “*In vitro* release and biological activities of *Carum copticum* essential oil (CEO) loaded chitosan nanoparticles,” *International Journal of Biological Macromolecules* 81, 283-290. https://doi.org/10.1016/j.ijbiomac.2015.08.010

Fadiji, T., Rashvand, M., Daramola, M. O., and Iwarere, S. A. (2023). “A review on antimicrobial packaging for extending the shelf life of food,” *Processes* 11(2), article 590. https://doi.org/10.3390/pr11020590

Ferreira, R. R., Souza, A. G., Barbosa, R. F., Marciano, J. S., Marques, F. A., Mitra, S. K., and Rosa, D. S. (2023). “The synergistic effect of nanocellulose and nanocapsules into poly (butylene adipate-co-butylene terephthalate) films for active packaging,” *Food Packaging Shelf Life* 35, article 100996. https://doi.org/10.1016/j.fpsl.2022.100996

Ferreira, R. R., Souza, A. G., Quispe, Y. M., and Rosa, D. S. (2021). “Essential oils loaded-chitosan nanocapsules incorporation in biodegradable starch films: A strategy to improve fruits shelf life,” *International Journal of Biological Macromolecules* 188, 628-638. https://doi.org/10.1016/j.ijbiomac.2021.08.046

Feyzioglu, G., Cansu, and Tornuk, F. (2016). “Development of chitosan nanoparticles loaded with summer savory (*Satureja hortensis* L.) essential oil for antimicrobial and antioxidant delivery applications,” *LWT* 70, 104-110. https://doi.org/10.1016/j.lwt.2016.02.037

Garofalo, E., Di Maio, L., Scarfato, P., Vitiello, L., and Incarnato, L. (2025). "Mechanical recycling of poly (butylene succinate)/poly (lactide) blends: Assessment of film blowing processability and film performances after multiple extrusions," *Chemical Engineering Journal* 505, article 159823. https://doi.org/10.1016/j.cej.2025.159823

Garavand, F., Rouhi, M., Jafarzadeh, S., Khodaei, D., Cacciotti, I., Zargar, M., and Razavi, S. H. (2022). "Tuning the physicochemical, structural, and antimicrobial attributes of whey-based poly (l-lactic acid)(PLLA) films by chitosan nanoparticles," *Frontiers in Nutrition* 9, article 880520. https://doi.org/10.3389/fnut.2022.880520

Garcia-Salazar, G., Romero-Alatorre, D. F., de la Luz Zambrano-Zaragoa, M., Serrano-Mora, L. E., Vidal-Romero, G., and Quintanar-Guerrero, D. (2026). "Thymol-loaded chitosan nanoparticles: A new ionic gelation method using a venturi tube," *Journal of the Mexican Chemical Society*, article 2467. https://doi.org/10.29356/jmcs.v70i1.2467

Gasti, T., Dixit, S., Hiremani, V. D., Chougale, R. B., Masti, S. P., Vootla, S. K., and Mudigoudra, B. S. (2022). "Chitosan/pullulan based films incorporated with clove essential oil loaded chitosan-ZnO hybrid nanoparticles for active food packaging," *Carbohydrate Polymers* 277, article 118866. https://doi.org/10.1016/j.carbpol.2021.118866

Ge, X., Huang, X., Zhou, L., and Wang, Y. (2022). "Essential oil-loaded antimicrobial and antioxidant zein/poly (lactic acid) film as active food packaging," *Food Packaging and Shelf Life* 34, article 100977. https://doi.org/10.1016/j.fpsl.2022.100977

Ghaderi-Ghahfarokhi, M., Barzegar, M., Sahari, M. A., and Azizi, M. H. (2016). "Nanoencapsulation approach to improve antimicrobial and antioxidant activity of thyme essential oil in beef burgers during refrigerated storage," *Food and Bioprocess Technology* 9, 1187-1201.

Ghani, S., Barzegar, H., Noshad, M., and Hojjati, M. (2018). "The preparation, characterization and in vitro application evaluation of soluble soybean polysaccharide films incorporated with cinnamon essential oil nanoemulsions," *International Journal of Biological Macromolecules* 112(2018), 197-202. https://doi.org/10.1016/j.ijbiomac.2018.01.145

Gomathi, T., Sudha, P. N., Florence, J. A. K., Venkatesan, J., and Anil, S. (2017). "Fabrication of letrozole formulation using chitosan nanoparticles through ionic gelation method," *International Journal of Biological Macromolecules* 104, 1820-1832. https://doi.org/10.1016/j.ijbiomac.2017.01.147

Hadidi, M., Pouramin, S., Adinepour, F., Haghani, S., and Jafari, S. M. (2020). "Chitosan nanoparticles loaded with clove essential oil: Characterization, antioxidant and antibacterial activities," *Carbohydr. Polym.* 236, article 116075. https://doi.org/10.1016/j.carbpol.2020.116075

Hajibonabi, A., Yekani, M., Sharifi, S., Nahad, J. S., Dizaj, S. M., and Memar, M. Y. (2023). "Antimicrobial activity of nanoformulations of carvacrol and thymol: New trend and applications," *OpenNano* 13, article 100170. https://doi.org/10.1016/j.onano.2023.100170

Hajirostamloo, B., Molaveisi, M., Jafarian Asl, P., and Rahman, M. M. (2023). "Novel soy protein isolate film containing cardamom essential oil microcapsules: Study of physicochemical properties and its application in Iranian white cheese packaging," *Journal of Food Measurement and Characterization* 17(1), 324-336.

Hanipa, M. A. F., Zaidi, S. A. S., Ishak, W. H. W., and Sajab, M. S. (2026). "Effect of cellulose nanofibrils in direct melt-blending of poly-(lactic acid) and poly (butylene succinate) for 3D printing," *BioResources* 21(1), 1050-1064. https://10.15376/biores.21.1.1050-1064

Hasani, S., Ojagh, S. M., and Ghorbani, M. (2018). "Nanoencapsulation of lemon essential oil in Chitosan-Hicap system. Part 1: Study on its physical and structural characteristics," *International Journal of Biological Macromolecules* 115, 143-151. https://doi.org/10.1016/j.ijbiomac.2018.04.038

Hasheminejad, N., Khodaiyan, F., and Safari, M. (2019). "Improving the antifungal activity of clove essential oil encapsulated by chitosan nanoparticles," *Food Chemistry* 275, 113-122. https://doi.org/10.1016/j.foodchem.2018.09.085

Herdiana, Y., Febrina, E., Nurhasanah, S., Gozali, D., Elamin, K. M., and Wathoni, N. (2024). "Drug loading in chitosan-based nanoparticles," *Pharmaceutics* 16(8), article 1043. https://doi.org/10.3390/pharmaceutics16081043.

Huang, S., Li, B., Huang, S., Wang, Y., Zhang, L., Li, J., and Yin, X. (2023). "Design and fabrication of bio-based functional composite materials with antibacterial, antioxidant, and improved mechanical properties based on poly (butylene adipate-co-terephthalate)(PBAT) for food packaging," *European Polymer Journal* 200, article 112492. https://doi.org/10.1016/j.eurpolymj.2023.112492

Jiang, S., Jia, W., Azmi, L. H. M., Sun, H., and Li, Y. (2025). "Highly effective antimicrobial films for food packaging using *Schisandra chinensis* extract and uncovering the contributing components via a novel deep learning approach," *Food Packaging and Shelf Life* 52, article 101636. https://doi.org/10.1016/j.fpsl.2025.101636

Kaboudi, Z., Peighambardoust, S. H., Nourbakhsh, H., and Soltanzadeh, M. (2023). "Nanoencapsulation of Chavir (*Ferulago angulata*) essential oil in chitosan carrier: Investigating physicochemical, morphological, thermal, antimicrobial and release profile of obtained nanoparticles," *International Journal of Biological Macromolecules* 237, article 123963. https://doi.org/10.1016/j.ijbiomac.2023.123963

Kalajahi, N. J., Ghanbarzadeh, B., Dehghannya, J., and Ostadrahimi, A. (2024). "The physicomechanical optimization and antimicrobial properties of the Ɛ-polylysine/ZnO nanoparticles loaded active packaging films," *Food and Humanity* 3, article 100401. https://doi.org/10.1016/j.foohum.2024.100401

Karam, T. K., Ortega, S., Nakamura, T. U., Auzély-Velty, R., and Nakamura, C. V. (2020). "Development of chitosan nanocapsules containing essential oil of *Matricaria chamomilla* L. for the treatment of cutaneous leishmaniasis," *International Journal of Biological Macromolecules* 162, 199-208. https://doi.org/10.1016/j.ijbiomac.2020.06.149

Kargarzadeh, H., Huang, J., Lin, N., Ahmad, I., Mariano, M., Dufresne, A., and Gałęski, A. (2018). "Recent developments in nanocellulose-based biodegradable polymers, thermoplastic polymers, and porous nanocomposites," *Progress in Polymer Science* 87, 197-227. https://doi.org/10.1016/j.progpolymsci.2018.07.008

Kazeminia, M., Gandomi, H., Koohi, M. K., Noori, N., Khanjari, A., and Ehterami, A. (2024). "Optimization of *Ziziphora clinopodioides* L. essential oil nanoencapsulation in chitosan nanocomplex by response surface methodology," *International Journal of Biological Macromolecules* 265, article 131114. https://doi.org/10.1016/j.ijbiomac.2024.131114

Keawchaoon, L., and Yoksan, R. (2011). "Preparation, characterization and *in vitro* release study of carvacrol-loaded chitosan nanoparticles," *Colloids and surfaces B: Biointerfaces* 84(1), 163-171. https://doi.org/10.1016/j.colsurfb.2010.12.031

Kennouche, S., Le Moigne, N., Kaci, M., Quantin, J. C., Caro-Bretelle, A. S., Delaite, C., and Lopez-Cuesta, J. M. (2016). "Morphological characterization and thermal properties of compatibilized poly (3-hydroxybutyrate-co-3-hydroxyvalerate) (PHBV)/poly (butylene succinate)(PBS)/halloysite ternary nanocomposites," *European Polymer Journal* 75, 142-162. https://doi.org/10.1016/j.eurpolymj.2015.12.009

Kirichenko, M. N., Kovalenko, K. V., Krivokhizha, S. V., Lobanov, A. N., and Chaikov, L. L. (2021). "New technique for identifying butter adulteration with palm fat by the DLS method," *Bulletin of the Lebedev Physics Institute* 48, 181-185.

Kowalczyk, A., Przychodna, M., Sopata, S., Bodalska, A., and Fecka, I. (2020). "Thymol and thyme essential oil—new insights into selected therapeutic applications," *Molecules* 25(18), article 4125. https://doi.org/10.3390/molecules25184125

Król-Morkisz, K., and Pielichowska, K. (2019). "Thermal decomposition of polymer nanocomposites with functionalized nanoparticles," in: *Polymer Composites with Functionalized Nanoparticles*, Elsevier, Amsterdam, Netherlands, pp. 405-435. https://doi.org/10.1016/B978-0-12-814064-2.00013-5

Kumar, S. P., Birundha, K., Kaveri, K., and Devi, K. T. R. (2015). "Antioxidant studies of chitosan nanoparticles containing naringenin and their cytotoxicity effects in lung cancer cells," *International Journal Biological Macromolecules* 78(2015), 87-95. https://doi.org/10.1016/j.ijbiomac.2015.03.045

Lanciu Dorofte, A., Dima, C., Ceoromila, A., Botezatu, A., Dinica, R., Bleoanca, I., and Borda, D. (2023). "Controlled release of β-CD-encapsulated thyme essential oil from whey protein edible packaging," *Coatings*, 13(3), article 508. https://doi.org/10.3390/coatings13030508

Laorenza, Y., and Harnkarnsujarit, N. (2021). "Carvacrol, citral and α-terpineol essential oil incorporated biodegradable films for functional active packaging of Pacific white shrimp," *Food Chemistry* 363, article 130252. https://doi.org/10.1016/j.foodchem.2021.130252

Laorenza, Y., Sablani, S. S., and Harnkarnsujarit, N. (2026). "Multilayer flexible lidding film prepared from TPS, citral, and PBAT: Mode of failure, mechanical behavior, and barrier properties," *Food Packaging and Shelf Life* 53, article 101683. https://doi.org/10.1016/j.fpsl.2025.101683

Li, B., Tang, T., Jiang, M., Chen, H., and Bai, Y. (2025). "Sustained-release electrospun films incorporated with oregano essential oil: Characterization, release kinetics and active packaging application for chicken breast," *Journal of Food Engineering* 2025, article 112760. https://doi.org/10.1016/j.jfoodeng.2025.112760

Li, X., Li, Z., Shen, J., Zheng, Z., and Liu, J. (2021). "Role of a nanoparticle network in polymer mechanical reinforcement: Insights from molecular dynamics simulations," *Physical Chemistry Chemical Physics* 23(38), 21797-21807.

Lu, W., Cui, R., Zhu, B., Qin, Y., Cheng, G., Li, L., and Yuan, M. (2021). "Influence of clove essential oil immobilized in mesoporous silica nanoparticles on the functional properties of poly (lactic acid) biocomposite food packaging film," *Journal of Materials Research and Technology* 11, 1152-1161. https://doi.org/10.1016/j.jmrt.2021.01.098

Mahmoud, N. M., Moneim, A. M. Y. A., Darweesh, O., El Zahaby, E. I., Elshaarawy, R. F., Hassan, Y. A., and Seadawy, M. G. (2024). "Fabrication and characteristics of new quaternized chitosan nanocapsules loaded with thymol or thyme essential oil as effective SARS-CoV-2 inhibitors," *RSC Advances* 14(40), 29330-29343. https://doi.org/10.1039/D4RA03298E

Manikandan, N. A., Pakshirajan, K., and Pugazhenthi, G. (2020). "Preparation and characterization of environmentally safe and highly biodegradable microbial polyhydroxybutyrate (PHB) based graphene nanocomposites for potential food packaging applications," *International Journal of Biological Macromolecules* 154, 866-877. https://doi.org/10.1016/j.ijbiomac.2020.03.084

Mao, J., Tang, Y., Zhao, R., Zhou, Y., and Wang, Z. (2019). "Preparation of nanofibrillated cellulose and application in reinforced PLA/starch nanocomposite film," *Journal of Polymers and Environment* 27, 728-738.

Matshetshe, K. I., Parani, S., Manki, S. M., and Oluwafemi, O. S. (2018). "Preparation, characterization and in vitro release study of β-cyclodextrin/chitosan nanoparticles loaded *Cinnamomum zeylanicum* essential oil," *International Journal of Biological Macromolecules* 118, 676-682. https://doi.org/10.1016/j.ijbiomac.2018.06.125

Mittal, R. P., Rana, A., and Jaitak, V. (2019). "Essential oils: An impending substitute of synthetic antimicrobial agents to overcome antimicrobial resistance," *Current Drug Targets* 20(6), 605-624. https://doi.org/10.2174/1389450119666181031122917

Mohamad, N., Mazlan, M. M., Tawakkal, I. S. M. A., Talib, R. A., Kian, L. K., and Jawaid, M. (2022). "Characterization of active polybutylene succinate films filled essential oils for food packaging application," *Journal of Polymers and Environment* 30(2), 585-596.

Oluoch, G., Matiru, V., Mamati, E. G., and Nyongesa, M. (2021). "Nanoencapsulation of thymol and eugenol with chitosan nanoparticles and the effect against *Ralstonia solanacearum*," *Advances in Microbiology* 11(12), 723-739. https://doi.org/10.4236/aim.2021.1112052

Omran, A. A. B., Mohammed, A. A., Sapuan, S. M., Ilyas, R. A., Asyraf, M. R. M., Rahimian Koloor, S. S., and Petrů, M. (2021). "Micro-and nanocellulose in polymer composite materials: A review," *Polymers* 13(2), article 231. https://doi.org/10.3390/polym13020231

Othman, S. H., Majid, N. A., Tawakkal, I. S. M. A., Basha, R. K., Nordin, N., and Shapi'i, R. A. (2019). "Tapioca starch films reinforced with microcrystalline cellulose for potential food packaging application," *Food Science and Technology* 39, 605-612.

Ozogul, Y., Karsli, G. T., Durmuş, M., Yazgan, H., Oztop, H. M., McClements, D. J., and Ozogul, F. (2022). "Recent developments in industrial applications of nanoemulsions," *Advances in Colloid and Interface Science* 304, article 102685. https://doi.org/10.1016/j.cis.2022.102685

Ozogul, Y., Karsli, G. T., Yazgan, H., Kuley, E., Oztop, H. M., Ozogul, F., and Esatbeyoglu, T. (2025). "Enhanced pathogen control through thymol and carvacrol nanoemulsions: A microfluidization approach," *Food and Bioprocess Technology* 18(6), 5377-5387.

Pant, A., and Negi, J. S. (2018). "Novel controlled ionic gelation strategy for chitosan nanoparticles preparation using TPP-β-CD inclusion complex," *European Journal of Pharmaceutical Sciences* 112, 180-185. https://doi.org/10.1016/j.ejps.2017.11.020.

Pasquina-Lemonche, L., Burns, J., Turner, R. D., Kumar, S., Tank, R., Mullin, N., and Hobbs, J. K. (2020). "The architecture of the Gram-positive bacterial cell wall," *Nature* 582(7811), 294-297.
Pastor, C., Sánchez-González, L., Marcilla, A., Chiralt, A., Cháfer, M., and González-Martínez, C. (2011). "Quality and safety of table grapes coated with hydroxypropylmethylcellulose edible coatings containing propolis extract," *Postharvest Biology and Technology* 60(1), 64-70.
Rajivgandhi, G., Kadaikunnan, S., Ramachandran, G., Chackaravarthi, G., Chelliah, C. K., Maruthupandy, M., and Li, W. J. (2023). "Anti-cancer ability of chitosan nanoparticles loaded plant essential oil evaluated against A549 human lung cancer cells through invitro approaches," *Journal of King Saud University-Science* 35(4), article 102598. https://doi.org/10.1016/j.jksus.2023.102598
Rajkumar, V., Gunasekaran, C., Dharmaraj, J., Chinnaraj, P., Paul, C. A., and Kanithachristy, I. (2020). "Structural characterization of chitosan nanoparticle loaded with *Piper nigrum* essential oil for biological efficacy against the stored grain pest control," *Pesticide Biochemistry and Physiology* 166, article 104566. https://doi.org/10.1016/j.pestbp.2020.104566.
Ramos, M., Beltran, A., Fortunati, E., Peltzer, M., Cristofaro, F., Visai, L., and Garrigós, M. C. (2020). "Controlled release of thymol from poly (lactic acid)-based silver nanocomposite films with antibacterial and antioxidant activity," *Antioxidants* 9(5), article 395. https://doi.org/10.3390/antiox9050395
Robledo, N., López, L., Bunger, A., Tapia, C., and Abugoch, L. (2018). "Effects of antimicrobial edible coating of thymol nanoemulsion/quinoa protein/chitosan on the safety, sensorial properties, and quality of refrigerated strawberries (*Fragaria* × *ananassa*) under commercial storage environment," *Food and Bioprocess Technology* 11(8), 1566-1574.
Rojas, A., Velásquez, E., Patiño Vidal, C., Guarda, A., Galotto, M. J., and López de Dicastillo, C. (2021). "Active PLA packaging films: effect of processing and the addition of natural antimicrobials and antioxidants on physical properties, release kinetics, and compostability," *Antioxidants* 10(12), article 1976. https://doi.org/10.3390/antiox10121976
Roy, S., M. Rahman, M. M., Ferdous, T., Likhon, M. N. A., and Sarwar Jahan, M. (2024). "Preparation of chitosan derivative and its application in papermaking," *International Journal of Biological Macromolecules* 256(Part 1), article 128371. https://doi.org/10.1016/j.ijbiomac.2023.128371
Russo, E., Gaglianone, N., Baldassari, S., Parodi, B., Cafaggi, S., Zibana, C., and Caviglioli, G. (2014). "Preparation, characterization and in vitro antiviral activity evaluation of foscarnet-chitosan nanoparticles," *Colloids and Surfaces B: Biointerfaces* 118, 117-125. https://doi.org/10.1016/j.colsurfb.2014.03.037
Sáez-Orviz, S., Marcet, I., Weng, S., Rendueles, M., and Díaz, M. (2020). "PLA nanoparticles loaded with thymol to improve its incorporation into gelatine films," *Journal of Food Engineering* 269, article 109751. https://doi.org/10.1016/j.jfoodeng.2019.109751
Safer, A. M., and Leporatti, S. (2021). "Chitosan nanoparticles for antiviral drug delivery: A novel route for COVID-19 treatment," *International Journal of Nanomedicine* 2021, 8141-8158.
Saifullah, M., Ahsan, A., and Shishir, M. R. I. (2016). "Production, stability and application of micro-and nanoemulsion in food production and the food processing

industry," in: *Emulsions*, Academic Press, pp. 405-442. https://doi.org/10.1016/B978-0-12-804306-6.00012-X

Sharma, K., Munjal, M., Sharma, R. K., and Sharma, M. (2023). "Thymol encapsulated chitosan-Aloe vera films for antimicrobial infection," *International Journal of Biological Macromolecules* 235, article 123897. https://doi.org/10.1016/j.ijbiomac.2023.123897

Shen, M., Song, B., Zeng, G., Zhang, Y., Huang, W., Wen, X., and Tang, W. (2020). "Are biodegradable plastics a promising solution to solve the global plastic pollution?," *Environmental Pollution* 263, article 114469. https://doi.org/10.1016/j.envpol.2020.114469

Shetta, A., Kegere, J., and Mamdouh, W. (2019). "Comparative study of encapsulated peppermint and green tea essential oils in chitosan nanoparticles: Encapsulation, thermal stability, *in-vitro* release, antioxidant and antibacterial activities," *International Journal of Biological Macromolecules* 126, 731-742. https://doi.org/10.1016/j.ijbiomac.2018.12.161.

Silva, N. C., Chevigny, C., Domenek, S., Almeida, G., Assis, O. B. G., and Martelli-Tosi, M. (2025). "Nanoencapsulation of active compounds in chitosan by ionic gelation: Physicochemical, active properties and application in packaging," *Food Chemistry* 463, article 141129. https://doi.org/10.1016/j.foodchem.2024.141129

Sivaram, S., Somanathan, H., Kumaresan, S. M., and Muthuraman, M. S. (2022). "The beneficial role of plant based thymol in food packaging application: A comprehensive review," *Applied Food Research* 2(2), article 100214. https://doi.org/10.1016/j.afres.2022.1002141

Soltanzadeh, M., Peighambardoust, S. H., Ghanbarzadeh, B., Mohammadi, M., and Lorenzo, J. M. (2021). "Chitosan nanoparticles encapsulating lemongrass (*Cymbopogon commutatus*) essential oil: Physicochemical, structural, antimicrobial and *in-vitro* release properties," *International Journal of Biological Macromolecules* 192, 1084-1097. https://doi.org/10.1016/j.ijbiomac.2021.10.070

Sotelo-Boyás, M. E., Correa-Pacheco, Z. N., Bautista-Baños, S., and Corona-Rangel, M. L. (2017). "Physicochemical characterization of chitosan nanoparticles and nanocapsules incorporated with lime essential oil and their antibacterial activity against food-borne pathogens," *LWT* 77, 15-20. https://doi.org/10.1016/j.lwt.2016.11.022

Su, S., Kopitzky, R., Tolga, S., and Kabasci, S. (2019). "Polylactide (PLA) and its blends with poly (butylene succinate)(PBS): A brief review," *Polymers* 11(7), article 1193. https://doi.org/10.3390/polym11071193

Sultan, M., Abdelhakim, A. A., Nassar, M., and Hassan, Y. R. (2023). "Active packaging of chitosan film modified with basil oil encapsulated in silica nanoparticles as an alternate for plastic packaging materials," *Food Bioscience* 51, article 102298. https://doi.org/10.1016/j.fbio.2022.102298

Sun, F., Zhao, J., Shan, P., Wang, K., Li, H., and Peng, L. (2024). "Gelatin-based composite film integrated with nanocellulose and extract-metal complex derived from coffee leaf for sustainable and active food packaging," *Food Hydrocolloids* 159, article 110610. https://doi.org/10.1016/j.foodhyd.2024.110610

Talebi, F., Misaghi, A., Khanjari, A., Kamkar, A., Gandomi, H., and Rezaeigolestani, M. (2018). "Incorporation of spice essential oils into poly-lactic acid film matrix with the aim of extending microbiological and sensorial shelf life of ground beef," *LWT* 96, 482-490. https://doi.org/10.1016/j.lwt.2018.05.067

Tan, J. M., Cui, R., Hu, T. G., Li, X. X., and Wu, H. (2025). "Preparation of chitosan/ shellac nanoparticles-essential oil Pickering emulsion active film and its application in bread preservation," *Food Packaging and Shelf Life* 49, article 101496. https://doi.org/10.1016/j.fpsl.2025.101496

Tawakkal, I. S. M. A., Cran, M. J., and Bigger, S. W. (2016). "Release of thymol from poly (lactic acid)-based antimicrobial films containing kenaf fibres as natural filler," *LWT-Food Science and Technology* 66(2016), 629-637. https://doi.org/10.1016/j.lwt.2015.11.011

Tosi, M. M., Ramos, A. P., Esposto, B. S., and Jafari, S. M. (2020). "Dynamic light scattering (DLS) of nanoencapsulated food ingredients," in: *Characterization of Nanoencapsulated Food Ingredients*, Academic Press, Cambridge, MA, USA, pp. 191-211. https://doi.org/10.1016/B978-0-12-815667-4.00006-7

Vahedikia, N., Garavand, F., Tajeddin, B., Cacciotti, I., Jafari, S. M., Omidi, T., and Zahedi, Z. (2019). "Biodegradable zein film composites reinforced with chitosan nanoparticles and cinnamon essential oil: Physical, mechanical, structural and antimicrobial attributes," *Colloids and Surfaces B: Biointerfaces* 177, 25-32. https://doi.org/10.1016/j.colsurfb.2019.01.045

Velderrain-Rodríguez, G. R., Acevedo-Fani, A., González-Aguilar, G. A., and Martín-Belloso, O. (2019). "Encapsulation and stability of a phenolic-rich extract from mango peel within water-in-oil-in-water emulsions," *Journal of Functional Foods* 56, 65-73. https://doi.org/10.1016/j.jff.2019.02.045

Vorawongsagul, S., Pratumpong, P., and Pechyen, C. (2021). "Preparation and foaming behavior of poly (lactic acid)/poly (butylene succinate)/cellulose fiber composite for hot cups packaging application," *Food Packaging and Shelf Life* 27, article 100608. https://doi.org/10.1016/j.fpsl.2020.100608

Wang, J., Ma, W., and Wang, X. (2021). "Insights into the structure of *Escherichia coli* outer membrane as the target for engineering microbial cell factories," *Microbial Cell Factories* 20(1), article 73.

Wang, X., Hu, Y., Zhang, Z., and Zhang, B. (2022). "The application of thymol-loaded chitosan nanoparticles to control the biodeterioration of cultural heritage sites," *Journal of Cultural Heritage* 53, 206-211. https://doi.org/10.1016/j.culher.2021.12.002

Wang, Y., Li, L., and Hu, J. (2023). "Development of biobased multifunctional films incorporated with essential oils@ polydopamine nanocapsules for food preservation applications," *International Journal of Biological Macromolecules* 253, article 127161. https://doi.org/10.1016/j.ijbiomac.2023.127161

Wang, X., Xue, Z., Sun, Y., Peng, B., Wu, C., and Kou, X. (2024). "Chitosan-ginger essential oil nanoemulsions loaded gelatin films: A biodegradable material for food preservation," *International Journal of Biological Macromolecules* 280, article 135791. https://doi.org/10.1016/j.ijbiomac.2024.135791

Wang, Y., Zhang, Y., Ma, Y., Liu, J., Zhang, R., and Zhao, J. (2025). "Preparation and application of chitosan/nano-TiO_2/daisy essential oil composite films in the preservation of *Actinidia arguta*," *Food Chemistry: X*, 26, article 102303. https://doi.org/10.1016/j.fochx.2025.102303

Wongphan, P., Nampanya, P., Chakpha, W., Promhuad, K., Laorenza, Y., Leelaphiwat, P., Bumbudsanpharoke, N., Sodsai, J., Lorenzo, J. M., and Harnkarnsujarit, N. (2023). "Lesser galangal (*Alpinia officinarum* Hance) essential oil incorporated biodegradable PLA/PBS films as shelf-life extension packaging of cooked rice," *Food Packaging and Shelf Life* 37, article 101077. https://doi.org/10.1016/j.fpsl.2023.101077

Wu, Y., Tang, Q., Yang, F., Xu, L., Wang, X., and Zhang, J. (2019). "Mechanical and thermal properties of rice straw cellulose nanofibrils-enhanced polyvinyl alcohol films using freezing-and-thawing cycle method," *Cellulose* 26, 3193-3204.

Yang, K., Liu, A., Hu, A., Li, J., Zen, Z., Liu, Y., and Li, C. (2021). "Preparation and characterization of cinnamon essential oil nanocapsules and comparison of volatile components and antibacterial ability of cinnamon essential oil before and after encapsulation," *Food Control* 123, article 107783. https://doi.org/10.1016/j.foodcont.2020.107783

Zabidi, N. A, Zainal, N. N., Intan Syafinaz Mohamed Amin Tawakkal, Mohd Salahuddin Mohd Basri, Siti Hajar Ariffin, and Mohd Nazli Naim. (2023). "Effect of thymol on properties of bionanocomposites from poly (lactic acid)/poly (butylene succinate)/ nanofibrillated cellulose for food packaging application," *International Journal of Biological Macromolecules* 251, article 126212. https://doi.org/10.1016/j.ijbiomac.2023.126212

Zhang, H., Li, X., and Kang, H. (2019). "Chitosan coatings incorporated with free or nano-encapsulated *Paulownia tomentosa* essential oil to improve shelf-life of ready-to-cook pork chops," *LWT* 116, article 108580. https://doi.org/10.1016/j.lwt.2019.108580

Zhang, H., Liang, Y., Li, X., and Kang, H. (2020). "Effect of chitosan-gelatin coating containing nano-encapsulated tarragon essential oil on the preservation of pork slices," *Meat Science* 166, article 108137. https://doi.org/10.1016/j.meatsci.2020.108137.

Zhao, X., Zhang, Y., Chen, L., Ma, Z., and Zhang, B. (2023). "Chitosan-thymol nanoparticle with pH responsiveness as a potential intelligent botanical fungicide against *Botrytis cinerea*," *Pesticide Biochemistry and Physiology* 195, article 105571. https://doi.org/10.1016/j.pestbp.2023.105571

Zhao, Y., Yao, G., Li, K., Ye, J., Chen, J., and Zhang, J. (2025). "Preparation, characterization, and antibacterial application of cross-linked nanoparticles composite films," *Food Chemistry: X* 25, article 102057. https://doi.org/10.1016/j.fochx.2024.102057

Ziaee, M., Sheikhzadeh Takabi, A., and Ebadollahi, A. (2023). "Fabrication of *Carum copticum* essential oil–loaded chitosan nanoparticles and evaluation its insecticidal activity for controlling *Rhyzopertha dominica* and *Tribolium confusum*," *Frontiers in Plant Science* 14, article 1187616. https://doi.org/10.3389/fpls.2023.1187616.

Zikeli, F., Vettraino, A. M., Biscontri, M., Bergamasco, S., Palocci, C., Humar, M., and Romagnoli, M. (2023). "Lignin nanoparticles with entrapped *Thymus* spp. essential oils for the control of wood-rot fungi," *Polymers* 15(12), article 2713. https://doi.org/10.3390/polym15122713

Article submitted: February 22, 2026; Peer review completed: May 2, 2026; Revised version received: June 17, 2026; Accepted: June 20, 2026; Published: July 14, 2026.
DOI: 10.15376/biores.21.3.8118-8156